CENTRO DE INVESTIGACIÓN CIENTÍFICA Y DE EDUCACIÓN SUPERIOR DE ENSENADA

PROGRAMA DE POSGRADO EN CIENCIAS EN ECOLOGÍA MARINA

Coastal algal blooms, the near-surface diurnal thermocline and wind transport toward the coast; ecological implications

Tesis

para cubrir parcialmente los requisitos necesarios para obtener el grado de Doctor en Ciencias

Presenta:

Mary Carmen Ruiz de la Torre

Ensenada, Baja California, 2013.

Abstract of the thesis presented by Mary Carmen Ruiz de la Torre as a partial requirement to obtain the Doctor in Science degree in Marine Ecology.

Coastal algal blooms, the near-surface diurnal thermocline and wind transport toward the coast; ecological implications

Abstract approved by:

_____

Dr. Helmut Maske Rubach
Director de Tesis

Algal blooms are a recurrent phenomenon of potentially socio-economic impact in many coastal waters including the upwelling region off northern Baja California, Mexico. A crucial question is why the blooms persist so long, considering the low growth rates in a highly dispersive environment. In coastal upwelling areas the diurnal wind pattern is directed towards the coast during the day. Above 5 m depth we regularly found positive Near Surface Temperature Stratification (NSTS), the resulting density stratification is expected to reduce the frictional coupling of the surface layer from deeper waters and allow for its more efficient wind transport. We propose that the net transport of the top layer of approximately 2.7 kilometers per day towards the coast helps maintain surface blooms of slow growing dinoflagellates such as *Lingulodinium polyedrum*. We measured: the near surface stratification with a free-rising CTD profiler, trajectories of drifter buoys with attached thermographs, wind speed and direction, velocity profiles via an Acoustic Doppler Current Profiler, Chlorophyll and cell concentration from water samples and vertical migration using sediment traps. The ADCP and drifter data show noticeable current shear within the first meters of the surface where temperature stratification and high cell densities of *L. polyedrum* were found during the day. Drifters with 1m depth drogue moved towards the shore, whereas drifters at 3 and 5m depth showed trajectories parallel or away from shore. A small part of the population extended diel vertical migration to the sea floor thus resisting horizontal dispersion at night. The persistent transport of the surface blooms towards shore should help maintain them in favorable environmental conditions with high nutrients, but also increase their potential socioeconomic impact. We studied the use of cell cycle information (Mitotic Index) to estimate the specific growth rate of the species dominating the observed bloom. To make the method applicable to field samples we considered the use of nuclear volume as a proxy for the DNA per cell. Culture results with this approach are promising but further investigation is needed.

Keywords: **Thermal stratification, wind transport, *Lingulodinium polyedrum***

Resumen de la tesis de Mary Carmen Ruiz de la Torre**,** presentada como requisito parcial para la obtención del grado de Doctor en Ciencias en Ecología Marina.

Coastal algal blooms, the near-surface diurnal thermocline and wind transport toward the coast: ecological implications

Resumen aprobado por:

_____

Dr. Helmut Maske Rubach
Director de Tesis

Los florecimientos algales densos son eventos recurrentes con gran impacto ecológico y socio-económico, y el conocimiento sobre su dinámica es aun escaso. Con la finalidad de contestar a la pregunta ¿Cómo se mantienen por periodos de tiempo largos los florecimientos de especies con tasas bajas de crecimiento en una zona hidrodinámicamente activa? El objetivo general de éste trabajo fue mostrar la relevancia del sistema de brisas y la estratificación superficial en el transporte de estos florecimientos. Para este estudio se midió la temperatura en los primeros 5 m de la columna de agua y el transporte de aguas superficiales durante un florecimiento algal denso dominado por el dinoflagelado *Lingulodninum polyedrum*. Se tomaron perfiles de temperatura, clorofila y absorción de luz con un CTD durante el mes de Octubre de 2011.Se cuantificó el movimiento de agua a partir de las trayectorias de tres cuerpos de deriva (1, 3 y 5 m) que tenían atados una cadena de termistores a las mismas profundidades y un GPS. Para verificar los comportamientos de los cuerpos de deriva, se compararon sus trayectorias con los datos obtenidos de un perfilador ADCP días antes de que comenzara el florecimiento; durante el florecimiento se colocaron además seis trampas de sedimento para cuantificar las células vegetativas que migran hasta el sedimento. Los resultados sugieren la presencia de una estratificación térmica y de densidad cerca de la superficie (1-3 m), mientras que el transporte de las aguas superficiales fue consistente con el arrastre por los vientos locales. Los datos de los cuerpos de deriva y ADCP mostraron ser compatibles y permitieron observar flujos cortantes en forma de espiral. En éste trabajo se discute que el transporte de las aguas superficiales de 2.7 km en ocho horas de brisa activa por día ayuda a mantener las condiciones ambientales favorables para que el florecimiento de dinoflagelados se mantenga. A pesar de que se encontró un bajo porcentaje de células que pudieran estar migrando al sedimento, se discute la importancia de éste comportamiento para entender la dinámica de dichos florecimientos Por otro lado, se estudió la posibilidad de estudiar el ciclo celular para estimar tasas de crecimiento específico de las especies observadas en campo, a partir del volumen del núcleo como proxi de la cantidad de ADN por célula. Los resultados de cultivos sugieren que el método propuesto tiene potencial, sin embargo se requiere de más investigación.

Palabras claves**: Estratificación térmica, brisas, *Lingulodinium polyedrum***

Dedicatoria

A los que hacen que mí día a día esté lleno de alegría, satisfacción y nuevos retos, a mi compañero de vida ***Hiram*** *y a mi amado hijo* ***Aarón*** *porque de la mano vamos sumando y construyendo un mejor futuro.*

Agradecimientos

Al **Centro de Investigación Científica y de Educación Superior de Ensenada** (CICESE) por otorgarme mi grado de Doctor en Ciencias.

Al **Consejo Nacional de Ciencia y Tecnología (CONACyT)** por el apoyo económico otorgado para la realización de mis estudios de Doctorado.

Al **Dr. Helmut Maske Rubach** por recibirme aquella tarde y poner a mi disposición una gama de temas interesantes de los cuales salieron mi tesis de Licenciatura y Maestría. Gracias por invitarme a participar en su proyecto del cual se desprende éste trabajo de tesis, por la confianza y por su invaluable guía. Gracias por estos 10 años no solo de enseñanza académica, sino por sus enseñanzas de vida y por supuesto por las horas de trabajo de plomería, carpintería y electrónica. Las frases ¨nada es fácil¨ y ¨siempre hay un momento para mejorar¨ estarán presentes para toda mi vida.

Al **Dr. José Luis Ochoa de la Torre** por aceptar ser parte de mi comité, por su paciencia con mi Matlab y vectores, gracias por siempre estar en la mejor disposición para ayudarme.

Al **Dr. Axayácatl Rocha Olivares** por sus comentario acertados y empuje para que éste trabajo estuviera terminado en tiempo y forma, por tener siempre su puerta abierta para cualquier duda.

Al **Dr. Ramón Cajal Medrano** por todas sus enseñanzas, comentarios y por su crítica constructiva. Gracias por su apoyo en los momentos más difíciles durante mi formación.

Thank you to **Dr. Dave Caron** for his support during this process. Thank a lot for your time, trust and comments.

Al **M.C. César Almeda Jauregui (COAJ**) compañero desde mi llegada al laboratorio, mi brazo derecho en el lab y mi confidente en los momentos de mayor estrés, gracias César por todas las palabras de aliento, por toda tu ayuda y por la amistad de 10 años.

Éste proceso de aprendizaje no sería posible sin la convivencia diaria con personas que hasta cierto punto comparten tus mismos intereses o gusto por la ciencia. Gracias a mis compañeros y amigos del Laboratorio de Microbios Marinos (MICMAR), por las horas de trabajo, de diversión, de llanto, de campo. A **Catalina Gutiérrez Paz** por tu amistad, apoyo y por darme la oportunidad de compartir mis conocimientos adquiridos en el laboratorio A **Ricardo Cruz López** por todo lo aprendido juntos. A **Josué Villegas Mendoza** por tu apoyo y tus buenos y atinados comentarios. A todos muchas gracias!

A **NortekUSA** por otorgarme el premio que hizo posible mis mediciones con el ADCP y por el apoyo económico para participar en la reunión de la AGU-2012. En particular al

M.C. Gerardo Silva por todo su apoyo y soporte para agilizar los trámites y a **Arturo Ocampo** por la ayuda (ADCP tips)

A la **Segunda Región Naval de la Secretaría de Marina de México (SEMAR**) y al personal de su estación meteorológica por facilitarme lo datos de viento utilizados en este trabajo; a **Santiago Higareda Cervera**, encargado de la estación meteorológica del CICESE por proporcionarme los datos meteorológicos.

A la **Dra. Christina Band Schmidt** por su apoyo y enseñanzas durante mi estancia en su laboratorio. Al **Dr. José Luis Peña Manjarrez** por las porras, apoyo incondicional y por compartir el entusiasmo que nos causan las mareas rojas. Al **Dr. Ernesto García Mendoza**, y a su equipo estrella de **FICOTOX** por mostrarme lo que hay más allá de *Lingulodinium.* A los miembros del laboratorio del Dr. Dave Caron en la USC, los Angéles, California por todo su apoyo durante mi estancia.

A los que están tras bambalinas y hacen posible que nuestra vida como estudiante sea más sencilla, mis queridas **Elizabeth Farías** y **Elvia Serrano**; a los caballeros nocturnos que cuidaron de mis estancias por la noche en el laboratorio, **Don Arthur** y **Don Jesús**; a **Don Rafa** por su alegre bienvenida cada mañana. A **Iván Castro Navarro** por ayudarme a perseguir mis boyas de deriva durante los muestreos para mi tesis. Al **Sr. Alfredo Ruiz**, por siempre estar pendiente de mis cheques. A **Francisco J Ponce** y **José Ma. Domínguez** por su apoyo técnico para la impresión de mis Posters. A **Ricardo Solís** por todo su apoyo técnico para echar a andar nuestros ¨juguetes científicos¨.

A mis profesores quienes dejan huella por su entusiasmo (amor al arte) y calidad académica **Dra. Sharon Herzka Llona, Dr. Juan Carlos Herguera y M.C. Vicente Ferreira.**

Al Departamento de Servicios Escolares en especial a **Dolores Sarracino**, **Citlalli Romero**, **Ivonne Best** y **Norma Fuentes** por todo su apoyo para realizar mis trámites académicos durante estos años. A **Lupita Morales y Ceci González** de la Biblioteca por su apoyo y compresión con mi mala memoria.

A la **Dirección de Estudios de Posgrado**, a la **División de Oceanología**, al **Posgrado en Ecología Marina** y al **Departamento de Oceanografía Biológica** por el apoyo económico otorgado durante la etapa final de la tesis. A los **miembros del CPP** por escuchar y apoyar mis solicitudes durante mi doctorado.

A mis queridas amigas que me acompañaron en éste proceso **Ruth Gingold** y **Karina de la Rosa** las quiero y las recuerdo siempre.

A mi amiga **Ana María Ramírez** por las horas-sacrificio con Matlab y otros asuntos, a **Ivonne Santiago** y **Guadalupe Cabrales** por todo su incondicional apoyo. A mis compañeros, gracias por los momentos compartidos**: Andrea, Nancy, Erick, Érica, Lorena Guerrero, Giovanna y Kena.** Al **Dr. Reginaldo Durazo** y **Dra, Lorena Linacre** por su amistad, apoyo y enseñanzas. A **Leonardo de la Rosa** por su sincera amistad.

Finalmente, pero no menos importante, quiero agradecer profundamente a los responsables de mi amor por la naturaleza, a los que me apoyaron desde el primer momento en que decidí ser Oceanóloga, a mis padres **Raimundo** y **Mary Carmen** por su confianza y apoyo incondicional; por inculcarme el amor a lo que uno hace. A mis hermanas **Adriana** y **Fernanda,** y a mi sobrina **Scarlett** por su cariño a pesar de la distancia. A mí adorada familia Poblana: Luna de la Torre, de la Torre Cruz y Corro, y Rivera de la Torre. A mi hermosa familia **Rivera Huerta** y **Rivera Arévalo** por su apoyo incondicional y amor, sin su ayuda ésto no hubiera sido posible. A mi familia de Ensenada: **Fam Vega Osuna**; y mis amigos-hermanos y sus familias **Diego**, **Jimena**, **Jhanely, Brenda, Mara, Eduardo y Fam Seinger Arredondo.** A los que de lejos me siguen recordando y apoyando con su amistad y cariño: **Dario** y **Angélica Félix**. ¡Los quiero!

A mi tan deseado ***Lingulodium polyedrum***, por aparecer cuando más te necesitaba, al océano y a sus maravillosos microbios por hacer de mi investigación un reto diario.

MUCHAS GRACIAS!

Index

List of Figures

List of Tables

Sinopsis

Los florecimientos algales densos son eventos recurrentes con alto impacto ecológico y socio-económico en aguas costeras mundiales. La región de surgencia de Baja California, México es una de estas regiones. Este estudio surge con la finalidad de contestar a la pregunta ¿Cómo se mantienen por periodos de tiempo largos los florecimientos, a pesar de ser especies con baja tasa de crecimiento y ocurrir en una zona hidrodinámicamente activa? El objetivo general de éste trabajo es mostrar la relevancia del sistema de brisas y la estratificación superficial en el transporte de estos florecimientos Termoclinas someras, de ~1 a ~2 m debajo de la superficie, asociadas al ciclo de radiación solar diurno han sido suficientemente reportadas y estudiadas. Es de esperarse que esta capa cuasi-homogénea, entre la superficie y la termoclina somera diurna, juegue un papel crucial en los intercambios entre el océano y la atmosfera. En regiones de surgencia costera, las brisas, dominadas por la diferencia térmica entre tierra y océano, están dirigidas hacia la costa durante las horas en que se espera la formación de la capa superficial diurna. Este trabajo se basa en la hipótesis que el gradiente de densidad de la termoclina somera es suficiente para reducir la fricción turbulenta y desacoplar la capa superficial diurna del resto de la columna de agua .El desacoplamiento facilitará el transporte de la capa superficial por el esfuerzo del viento y como consecuencia, el transporte integral de la capa estará dirigido hacia la costa pues. Como resultado se espera que las aguas superficiales y las poblaciones de fitoplancton asociadas, sean transportadas hacia la costa. No se encontró en la literatura una referencia sobre un mecanismo similar a lo propuesto en nuestra hipótesis. Otro elemento en la hipótesis incluye el fortalecimiento de la termoclina somera debido al incremento de turbidez, y en consecuencia de absorción de la radiación solar, durante la presencia de los florecimientos algales.

Para evaluar la importancia ecológica del transporte se ha buscado un método para estimar la tasa específica de crecimiento. El desarrollo del florecimiento depende de la relación entre dispersión física y crecimiento específico de especies que dominan durante mareas rojas. Sabemos que la estimación de la tasas de crecimiento específico de una especie en poblaciones naturales mixtas es difícil. Los métodos publicados son laboriosos y poco prácticos para procesar muchas muestras de campo. Con el objetivo de desarrollar una metodología para estimar las tasas de crecimiento se utilizaron indicadores del ciclo celular, por ejemplo el volumen nuclear para distinguir entre las fases G1 y G2 del ciclo celular.

En capítulo 1 de este trabajo se reportan los resultados obtenidos acerca de la formación de la capa superficial diurna y el transporte de aguas superficiales durante un florecimiento algal denso representado por el dinoflagelado *Lingulodinium polyedrum.* Los resultados obtenidos a partir de las temperaturas registradas por los termógrafos acoplados en los cuerpos de deriva sugieren la

ausencia de una capa homogénea en los primeros metros de la columna de agua; no se encontraron diferencias significativas entre los gradientes de 1 a 3 metros y aquellos de 3 a 5 metros (Figura 7). Contrario a lo que se esperaba la ausencia de una capa superficial diurna homogénea fue lo más común (Figura 9A). La presencia de una estratificación térmica significativamente positiva también se encontró en los perfiles donde se colocó el ADCP (Figura 10) y en una estación representativa de la región de surgencia (Figura 11). De hecho, muchos perfiles, más de la mitad, presentan la dificultad de definir, aun visualmente, la 'capa de mezcla'. Con respecto al transporte de aguas superficiales, los datos de los cuerpos de deriva con elementos de arrastre a 1, 3 y 5m fueron compatibles con los perfiles medidos por el ADCP (Figure 12). Los datos de corrientes muestran la presencia de un flujo cortante de superficie a profundidad en forma de espiral (Figure 13). Las trayectorias de las boyas superficiales fueron consistentes con el patrón de viento local para el mes de Octubre; en donde durante ocho horas de brisa continua, los cuerpos de deriva con elemento de arrastre a 1 metro, se trasladaron hacia la costa y los cuerpos de deriva con centro de arrastre a 5 metros se trasladaron hacia fuera de la costa o en dirección contraria al movimiento en superficie (Figura 15 y 17). Estos resultados sugieren que durante el día, los organismos próximos a superficie son eficientemente transportados hacia la costa, sin embargo no se encontró evidencia acerca del efecto del incremento en la concentración de los organismos, y en turbidez, en algún aumento de temperatura superficial como se esperaba. En la figura 18 los perfiles de temperatura dentro y fuera de las manchas muestran una diferencia de temperatura en los primeros metros, sin embargo si se observa más a detalle el gradiente entre 1 y 5 metros es similar entre los perfiles dentro y fuera de las manchas con florecimientos algales densos.

Dentro de los resultados, en las mediciones de velocidad a partir de las trayectorias de flotadores se observaron oscilaciones con ~20 minutos de periodo que fueron asociadas a la presencia de seiches en la Bahía (Figura 20). Estos resultados no se consideran relevantes para el transporte superficial, sin embargo se deben de considerar en el análisis de muestras de sedimento ya que se ha observado que dichas oscilaciones pueden tener un efecto en la re-suspensión de sedimento, lo cual es relevante si consideramos que células vegetativas de organismos que migran pueden utilizar el sedimento para adquirir nutrientes o que células en reposo (quistes) pueden ponerse en suspensión e iniciar la formación de un florecimiento algal denso.

En el capítulo II se presentan los avances acerca de la propuesta metodológica para estimar tasas de crecimiento específico en poblaciones naturales. Esta propuesta nace de la ausencia de una metodología robusta y práctica para estimar tasas de crecimiento específico en poblaciones mixtas. El método propuesto se basa en la información acerca del ciclo celular de cada especie, en este caso se trabajó con *Lingulodinium polyedrum* por ser una especie modelo con tasa de crecimiento lento y con un comportamiento de migración

vertical. El concepto del método se basa en la información del ciclo celular (Figura 21), se espera que el volumen del núcleo se pueda utilizar como un proxie del contenido de ADN. Esto no requiere la medición por fluorescencia que está asociada a varias complicaciones como se reportan en este trabajo. El método propuesto incluye el análisis de imágenes tomadas con microscopia de epifluorescencia a distintos niveles de enfoque para la reconstrucción 3D de núcleos teñidos con DAPI, y la estimación de proxies del volumen a partir de la geometría del núcleo. Los resultados preliminares mostraron que una de las principales consideraciones al teñir la muestra fue la estabilidad de la tinción de las células (Figura 28) y otra el daño a las células al momento del tratamiento (Figura 29). Dentro de los retos más relevantes están el poder adquirir el suficiente número de células para poder estimar el volumen del núcleo y para interpretar correctamente las tasas de crecimiento específicas considerar su relación con respecto al crecimiento sincronizado y la migración vertical de éstos organismos.

La información suplementaria presentada en este trabajo refiere a los resultados obtenidos en la prueba para documentar el movimiento de aguas superficiales a partir de imágenes fotográficas tomadas desde un punto alto. La principal limitación que se encontró fue delimitar en las imágenes de la bahía los parches del florecimiento con suficiente contraste y la dificultad de poder referenciar las imágenes para obtener datos cuantitativos acerca del transporte. Finalmente, este trabajo consideraba la obtención de datos experimentales sobre la migración vertical de *Lingulodinium polyedrum* para poder tener una interpretación más detallada acerca del florecimiento. Se espera que en futuros trabajo se pueda obtener dicha información con la finalidad de relacionarlos con lo encontrado sobre el trasporte de aguas superficiales y la estimación de tasas de crecimiento en campo.

CHAPTER I. Maintenance of coastal surface blooms by surface temperature stratification and wind drift

1. Introduction

In the last decades, dense algal blooms, historically often referred to as red or brown tides, have been studied worldwide because of their socioeconomical and ecological implications (Hallegraeff,1993; Lewitus et al 2012). The increasing frequency of blooms has been related to coastal eutrophication (Gilbert and Burkholder, 2006), climatic shifts (Hinder et al 2012), and the transport of algal species by ship ballast water (Anderson et al 2012). The spatial distribution of algal blooms is determined by the interaction between biological and ecological features of the organism on the one hand, and by physical oceanographic structures and processes on the other hand (McManus and Woodson, 2012). Despite a large number of publications related to coastal surface blooms, little is known about hydrographic conditions that promote their formation and maintenance (Hallegraeff, 1993; Gilbert et al 2005). Here, we consider oceanographic aspects of surface bloom transport, but the processes we describe are relevant for all surface water constituents, such as wastewater, nutrients or harmful algal bloom forming species, all of these having potentially socioeconomic impacts (Haase et al 2012).

Surface transport is determined by several factors, including coastal morphology, wind patterns and water column stratification. Thermal stratification is crucial in controlling the horizontal dynamics of the upper ocean at different scales (Gentemann and Minnett, 2008); figure 1 compares the near surface temperature stratification (NSTS) with sea surface temperature (SST) and the seasonal thermocline; these different components are controlled largely by the same meteorological conditions but at different time scales (Minnett, 2003). High solar

irradiance and low surface mixing rates promote stratification and the formation of a diurnal thermocline in clear ocean waters (Bissett et al 2001); during the day this thermocline is formed by solar heating close to the surface and the thickness of the surface layer increases, during night the thermal stratification is reduced due to surface cooling (Noh et al 2009). Note that the vertical scale of sea surface temperature is restricted to the first few centimeters and can be related to neuston organisms; here we are concerned with the more extensive vertical scale for surface blooms and NSTS (Figure 1). Vertical density structure defines the current shear pattern between the wind drift at the surface and the deeper water. With NSTS there can be significant difference in current bearings within few meter depth intervals, which can influence the distribution of phytoplankton (Gentien et al 2005). In coastal upwelling areas, alongshore wind is a dominant factor inducing Ekman drift directed offshore. The thermal wind breeze often associated with coastal upwelling has a direct influence on the dynamics of the surface mixed layer (Kudela et al 2005) and on the onshore transport of surface waters (Kaplan et al 2003; Tapia et al 2004; Pineda et al 2007). Sea breezes occur at two-third of earth coastlines (Simpson, 1994) and near 30° latitude are expected to generate near inertial oceanic motions (Hyder et al 2011).

This research was partially motivated by the recurrent formation of dense surface algal blooms in the coastal waters off Baja California, lasting from weeks to months. The dominant surface bloom organisms that make up red tides are slow growing dinoflagellates. Under favorable growth conditions their generation time is about 2 days (Smayda, 1997), which makes the persistence of these blooms more difficult to explain. Part of the explanation may relate to the dinoflagellate's diel vertical migration that is supposed to increase survival and competitive success (Cullen and Horrigan, 1981; McIntyre et al 1997).

Vertical migration involves geotaxis, a circadian rhythm and chemosensory behavior; the general pattern of these photosynthetic species is to move to

shallower depths during the day and to deeper waters at night for nutrient acquisition and predator avoidance. The specifics of this behavior depend on the species and environmental conditions. The vertical total migration can be about 16 m day^{-1} with vertical velocities up to 1-2 m h^{-1} or more (280-560 µm s^{-1}) (Burkholder et al, 2006). Typically, vertical migration extends down to the pycnocline or nutricline (Cullen, 1985; Townsend et al 2001); however, not all dinoflagellates show this pattern. For example, in the east coast of the United States, *Karenia brevis* has been shown to swim directly toward the sediment to acquire organic and inorganic nutrients from pore water to alleviate bottom-up controls and permit populations to persist as vegetative cells near the sediment–water interface (Sinclair and Kamykowski, 2008).

Our study was based on the assumption that diurnal near surface stratification together with the onshore wind contributes to the maintenance of surface blooms. NSTS was expected to reduce the frictional coupling with the lower water column thus facilitating the wind transport of the surface layer. The sea breezes in coastal upwelling areas such as the California current system are driven by the temperature gradient between the land and the sea and are directed towards the coast during daytime (Checkley and Barth, 2009; Hyder et al 2011). Our results show that near surface stratification is a common occurrence during the day in our coastal waters but the form of stratification is different from our initial concept of a homogenous near surface layer (Figure 1). We could document the expected transport of the surface bloom that should help slow growing dinoflagellates such as *Lingulodinium polyedrum* to maintain high cells densities closer to the coast during a prolonged time in a region with coastal and tidal currents, facilitating the permanence of dense algal blooms. The wind transport of the surface layer will have to be considered in the horizontal distribution of any dissolved and particulate constituent in this layer.

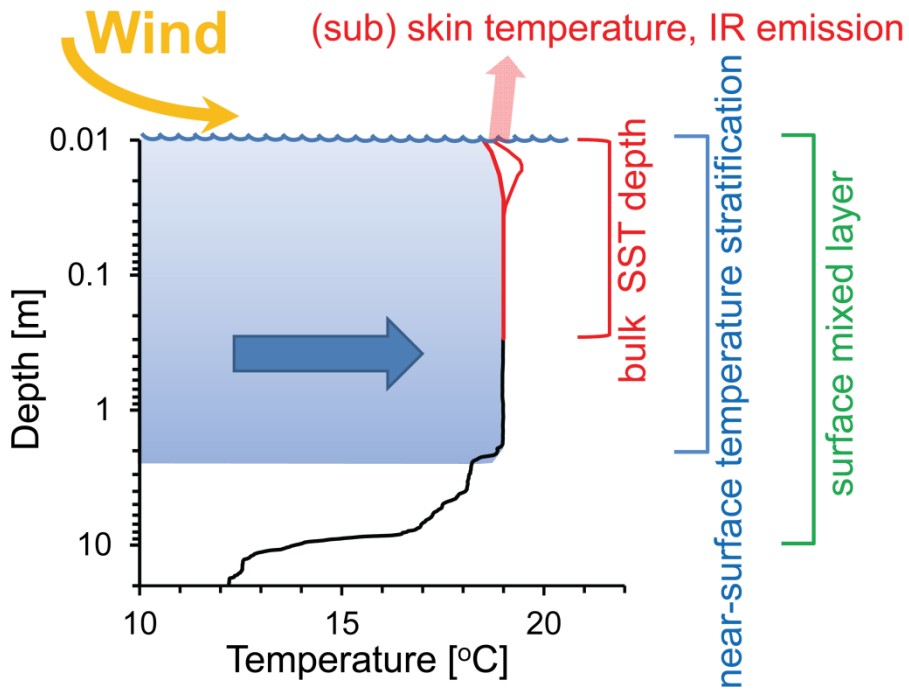

Figure 1 Schematic representation of different thermal stratification depth scales. Wind forcing (yellow arrow) induces the movement of the near surface layer (big arrow within the water column).

2. Material and Methods

2.1 Study site and water samples

The fieldwork was carried out in the Todos Santos Bay (TSB, 31º 40' to 31º 56'N and 116º36' to 116º 50'W) on the northwestern Baja California coast. TSB is an open coastal bay of approximately 10km diameter and two small islands located near the southwestern corner of the entrance. Surface water characteristics within the TSB are closely related to the cold California Current (Argote-Espinoza, 1991). Data for the present study were collected on October 4, 5, 6, 11, 12, and 18, 2011 during a *L. polyedrum* bloom. The sampling, profiling, and drifter deployment started at the time the bloom patches could be observed at the surface, about

10:00 am and finished when surface patches disappear (around 17:00 hrs.). Sampling locations were chosen depending on the detectability of patches (Figure 2). ADCP used to compare the performance of drifters were deployed during pre-bloom on September 21, 28 and 29, 2011. Sediment traps were deployed October 5, 11 and 18, 2011 at around 17:00 hrs. Additional CTD profiles were taken in a coastal site referred to as FLUCAR station that is near Ensenada and presents typical upwelling conditions (Linacre et al, 2012), temperature profiles were compared with the temperature profiles obtained during the bloom. Data obtained from FLUCAR station were taken on September 2, 22, 29 and 30, 2011.

Water samples were taken with Niskin bottle at 1, 3, 5, 10, 15m for chlorophyll, phytoplankton and bacterial counts on October 4, 5, 6, 11, 12, and 18, 2011. Samples were kept until return to the laboratory. Chlorophyll *a* was filtered on glass fiber filters (GFF, Whatman) with sample volumes from 0.01 to 0.5 l depending on sample concentration. The filtered samples were frozen at -40^{o}C until extraction with 90% Acetone at -20^{o}C for 24 hours and then measured with a fluorometer (Turner Design 10) according to Welschmeyer, 1994.

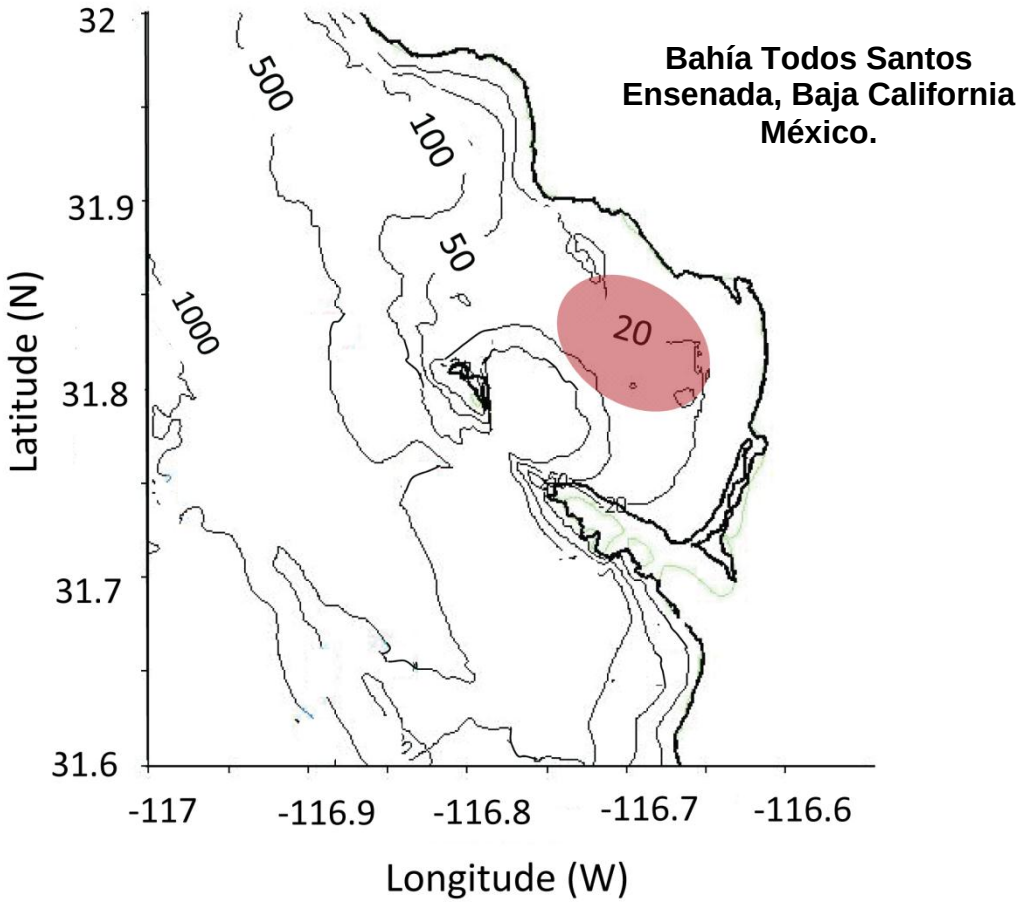

Figure 2 Study site, Todos Santos Bay. Baja California, Mexico (31o 40´ to 31o 56N and 116o 36´ to 116o 50´W). Circle indicates the bloom area.

2.2 Near surface thermal stratification

A free-rising CTD (Maske et al 2012) (Figure 3) was used to document the vertical structure of temperature in the water column up to 0.4 m below the surface with a nominal vertical resolution of 0.05 m. The profiler included sensors for temperature, conductivity, pressure (RBR), PAR (Biospherical), chlorophyll fluorescence and particle back scattering (Wetlabs). A comparison of the 0 to 5 m values of particle backscatter and chlorophyll fluorescence showed no near surface photoinhibition of the chlorophyll fluorescence (data not shown). The chlorophyll

fluorometer data were calibrated against extracted chlorophyll concentration measured in concomitantly sampled water ($R^2 = 0.8476$, $p<0.05$). A total of up to 15 vertical profiles per day were obtained during the 6 sampling days. To assess thermal stratification and to document the pattern of the formation of the superficial thermocline, three thermographs (Hobo U22 Pro V2) were attached at 1, 3 and 5m to each CODE-type drifter (Figure 4). Thermographs recorded water temperature every 5 minutes during the sampling period with 0.01^oC resolution and 0.2^oC accuracy. The thermographs were completely covered with one layer of white electric tape to avoid solar heating of the black thermograph body and to protect the communication window. To assure instrument comparability, temperature measurements started at least one hour before the deployment with all thermographs kept together in an icebox. A non-parametric test (Kruskal-Wallis), as implemented in Staitistica v. 7.1 was used to assess temperature difference among depths, and among drifters.

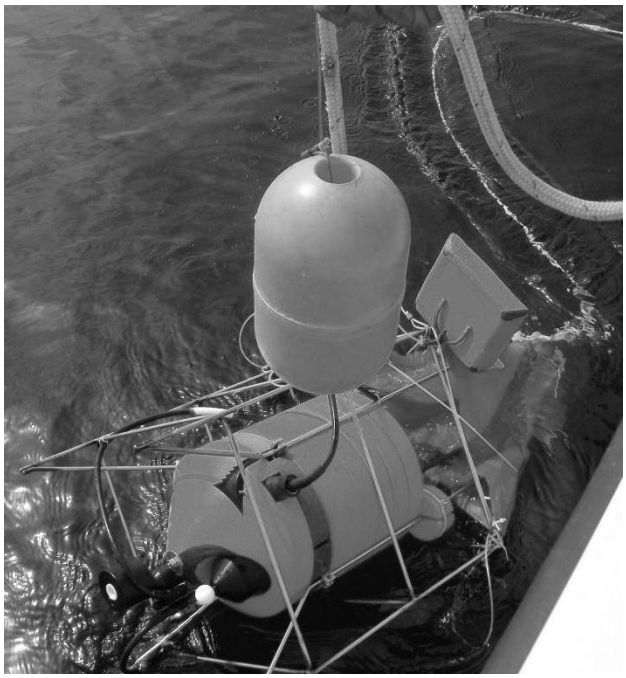

Figure 3 CTD profiler modified for free rising data acquisition

2.3 Horizontal water movement:

2.3.1 Drifter's deployments

To document the horizontal water movement, three CODE-type drifter buoys were deployed during the day. The projected drogue areas were 1 m^2 placed at 1, 3, or 5 m depth. To document the drifter´s trajectories, a GPS (Rino 110, Garmin) was attached to their surface buoy (Figure 4). GPS data were downloaded and processed using MapSource software version 6.16.3 (Garmin). The time and location of drifter deployment and recovery were registered. Two additional Holey Sock type drifters (1m diameter, 1m length) positioned at 1m and 5m depth were deployed together with the Code type drifters at the same depth. Holey sock type drifters did not have a GPS attached, but deployment and recovery locations and times were registered to compare both drifter types. We used Google Earth v6.2 to visualize and document the motion path pattern behavior of the three Code type drifters during the sampling period. Missing data are due to failure in data recording (October 11 and 12, at 3m depth and October 18 at 1 m depth).

2.3.2 ADCP and CODE type drifter comparison

Detailed comparisons of drifters' trajectories and ADCP velocities were done for three days, prior to the bloom. An Acoustic Doppler Current Profiler (ADCP) (Aquadopp Nortek, 1 MHz) was anchored, looking upward from 11 m depth and profiling close to the surface, in 21 0.5 m-thick layers. In the upper meter the surface reflection is expected to produce noise that is reduced by time integration. Considering the magnetic declination, the West to East (u) and South to North (v) currents were inferred with the ADCP in 2 min averages. Drifter-derived velocity was compared with the velocity measured by the ADCP at 1, 3 and 5 meters to evaluate their water following capability, or its degree of agreement with the ADCP measurements. Each drifter was deployed at approximately 250 meters from the

anchored ADCP and the drifter position was registered, via a GPS, every 5 minutes for at least 2 hours. The ADCP data and trajectories were obtained during September 2011 on the 2nd (13:30 to 15:30 hrs), 21st (14:10 to 15:40 hrs) and 29th (11:00 to 16:00 hrs).

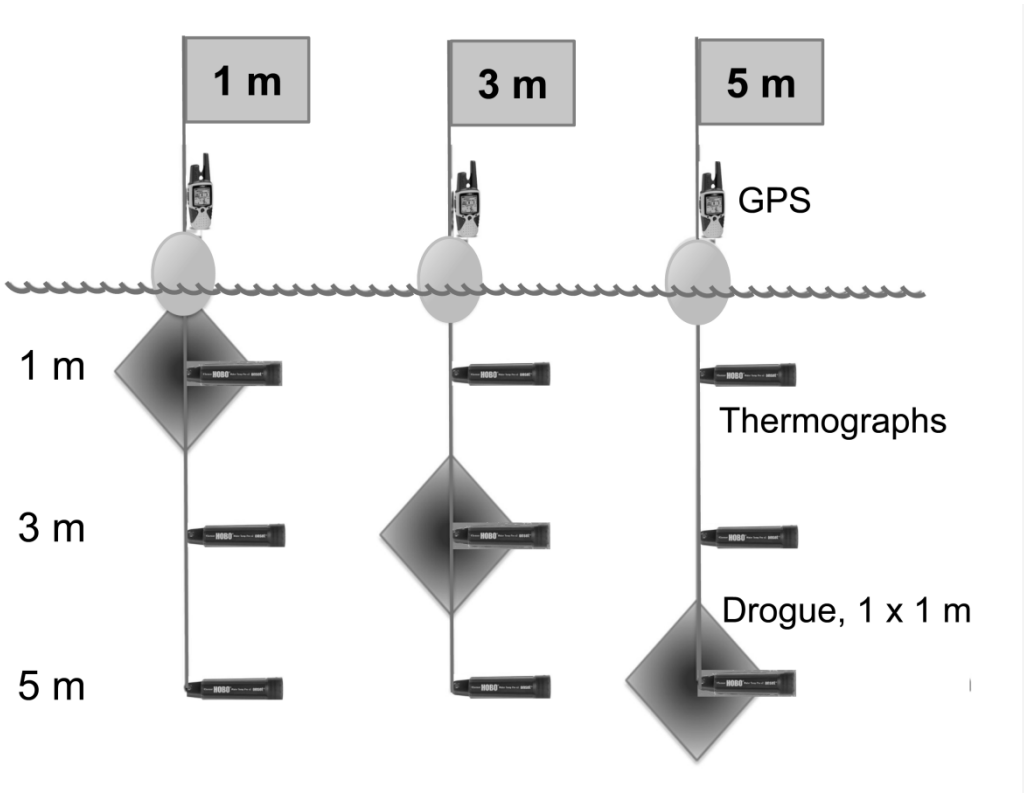

Figure 4 Schematic representations of CODE-type drifters. Each drifter consisted of flag, GPS attached above flotation (yellow ovals), kite type drogues of 1 m2 in two directions (blue diamond), and 3 thermographs at depths 1, 3 and 5 m.

Data comparison included: i) time series of velocities, by inferring drifter velocities based on their motion path, ii) inferred trajectories, by integration of ADCP velocities over time. In the latter, the virtual trajectories project particle trajectories according to measured velocity by the moored ADCP. In the first comparison the measured velocities are at different locations. Both comparisons make the assumption that the lateral scale of velocity variability is larger than the separation of drifters and current meter. Drifter and ADCP measurements were

compared during a non-bloom, low wind strength period, therefore these measurements are useful for comparisons but the data are not typical for bloom conditions.

2.3.3 Current and wind pattern measurements during the bloom

For each CODE type drifter deployed during the bloom, we used the latitude ($\phi = \phi(t)$) and longitude ($\lambda = \lambda(t)$) information, where t is time to calculate the West to East velocity, or $u = (R \cdot \cos\phi)^{-1} d\lambda / dt$, and the South to North velocity, or $v = R^{-1} d\phi / dt$, where R is the radius of the earth. The differentiation was approximated by centered finite differences using one sample before and another sample after the time of interest (i.e. $u(t_I) = (R \cdot \cos\phi_O)^{-1}(\lambda_{I+1} - \lambda_{I-1}) / (t_{I+1} - t_{I-1})$ and $v(t_I) = R^{-1}(\phi_{I+1} - \phi_{I-1}) / (t_{I+1} - t_{I-1})$, where the index I runs through the sequence of consecutive measurements, and $\phi_O = 31.847^O$, the latitude of the anchored ADCP). For each drifter position recorded during a deployment, we computed n^{-2} velocity vectors.

Virtual trajectories that follow from the ADCP recordings were computed as

$\lambda(t_I) = \lambda(t_{I-1}) + (R \cdot \cos\phi_O) u(t_I)(t_I - t_{I-1})$, and $\phi(t_I) = \phi(t_{I-1}) + R v(t_I)(t_{I+1} - t_{I-1})$.

To analyze the path of the drifters we plotted the drifter trajectories, after removal of outliers so the track was relatively smooth and continuous. We kept the part of the trajectories that coincided in time; removing all data prior to the entry of the last drifter into the water as well as all data after the first drifter was picked up. For the wind, we use here the direction of propagation, as opposed to the meteorological convention. Wind velocity and direction data from sampling period (04, 05,06,11,12 and 18 October, 2011) were obtained from a meteorological station maintained by the Navy Secretariat (SEMAR), located in its Oceanographic

station near the Port of Ensenada Baja California. Concurrent observations of October average wind intensity and direction were obtained from a meteorological station, managed by the Centro de Investigación Científica y de Educación Superior de Ensenada (CICESE), and located on shore less than 4 km from our observation point. The average of wind direction and velocity and its standard deviations were plotted during local solar time. Wind speed and wind direction for each sampling day were processed for the intervals of sea breeze peaks (13-15 hrs.) to compare with the velocities and trajectories of 1 and 5 m drifters during the bloom.

2.6 Assessment of vertical migration of *L. polyedrum*

Sedimentation of vegetative cells *L. polyedrum* cells was monitored by means of six sediment traps placed on the sea floor at approximately 14 m depth below surface bloom patches at about 16:30 hrs on October 5, 11, and 18, 2011. In order to fix the vegetative cells reaching the sediment, prior the deployment a mixture of chilled salt brine and $HgCl_2$ was added to three traps, and chilled salt brine was added to the other three traps .The traps were collected around 9:00 hrs, the next day. Each trap consisted of a black ABS tube (42 cm height, 10.7 cm diameter) with four inside baffles to avoid re-suspension of sample during recovery of the trap; the mouth of the trap was 0.55 m about the sea floor (Figure 5). Samples were kept dark and cold until arrival at the laboratory. Given the lack of statistically significant difference in average of cell abundance between traps with and without $HgCl_2$, we used all six traps to calculate sedimentation rates.

In the laboratory, a 250 ml subsample of the content of each trap was fixed with glutaraldehyde 1% final concentration to preserve red autofluorescence. In order to separate, re-suspend and mix sediment trap samples, the 20 ml aliquot was sonicated for 5 minutes. Then cells in suspension were counted in a 20 μl

glass counting chamber using an epifluorescence microscope (Zeiss Axioscope with a Xenon lamp) under blue light (450-490 nm excitation, dicroic 510 nm, >515 nm emission). Vegetative cells with red auto-fluorescence were easily distinguished from cyst with green auto-fluorescence (Figure 6). Cell abundance was regressed against the calibrated in situ chlorophyll fluorometer (R^2 = 0.7784, $p<0.05$) (Figure 7). The *in situ* fluorometer profile was then used to estimate the cells contained within the surface layer (from the surface down to 3 m depth). The abundance of the vegetative cells in the sediment traps allowed determining the daily percentage of migrating cells (cell m^{-2}) by comparing the abundance of vegetative cells counted in the traps (cell m^{-2}) with the cells contained in the near surface water column integrated from 0 to 3 m depth (cell m^{-2}).

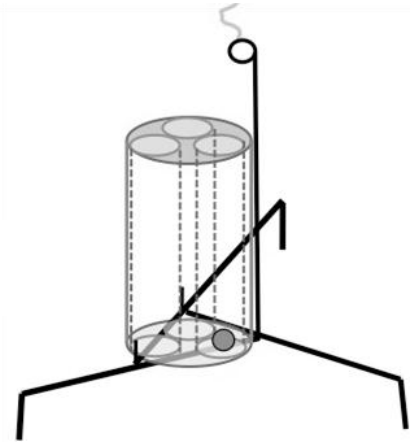

Figure 5 Schematic representation of the sediment trap used to collect down-migrating cells during a Lingulodinium polyedrum bloom. The gray disk at the bottom of one of the small tubing represents the glass balls used to check if the sediment trap had been turned over during the deployment.

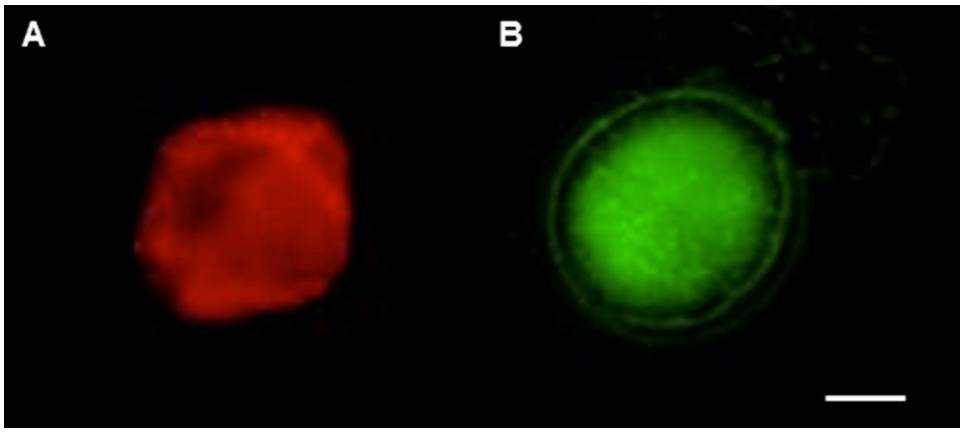

Figure 6 *Lingulodinium polyedrum* cells from sediment traps. Vegetative cells from sediment traps deployed on October 5, 2011. A. Vegetative cells with red chlorophyll autofluorescence (Ex. 450 nm, Em. 680 nm), B. Cyst cells with green autofluorescence (Ex. 495 nm, Em. 520 nm) objective 20X. Scale bar: 10 µm.

3. Results

3.1 Near surface temperature stratification (NSTS)

3.1.1 NSTS during the dense algal bloom

Temperatures within the surface layer were logged by three thermographs attached to each of the drifters at 1, 3 and 5 m depths. Data analysis indicated no differences ($p<0.05$) between thermographs at the same depth but attached to different drifters, and no clear trend during deployment, suggesting little horizontal differences in temperature structure and no strong diurnal cycle in temperature. There were significant differences in temperatures between 1 to 3 m and 3 to 5 m ($p<0.05$) (Figure 7). Thermograph temperature within the superficial layer were between 17.5 and 19^{o}C for October 4, 5, 6, 11 and 12; but for the last sampling date (October 18) the temperature decreased to between 15.5 and 18^{o} C. Temperature gradients did not increase during the day, implying that the

temperature gradient was already present when the bloom organisms arrived at the surface and the drifters where deployed. Temperature gradients were also density gradients; the average temperature differences (Figure 8) can be recalculated into SigmaT differences. SigmaT differences between 1 to 3 m represent 0.0775 [kg m^{-3}] and differences between 3 to 5 m represent 0.148 [kg m^3].

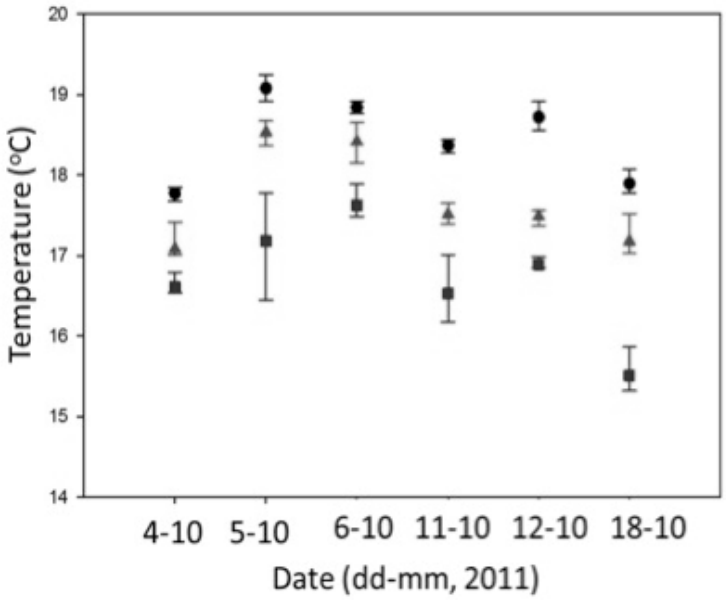

Figure 7 Temperature values registered by thermographs at 1 m (circles), 3 m (triangle) and 5 m (square) during the trajectories of CODE type drifters for each day of the sampling dates. The vertical bars represent the standard deviation of the temperature during deployment.

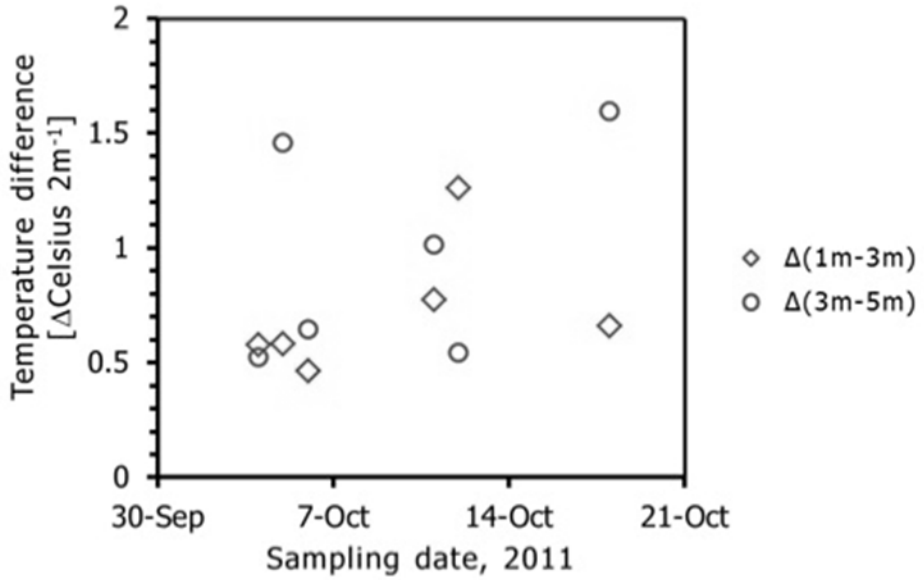

Figure 8 Average temperature difference within 2 m depth difference for sampling dates.

Typically the CTD profiles in the study site showed a linear decrease in temperature with depth and no marked temperature step identifying a thermocline that would separate a surface layer from the rest of the water column (Figure 9A). For our data, we used a qualitative definition of thermocline because common characterizations are cumbersome to apply (Fiedler, 2010) and our study depth is much smaller than typical oceanographic applications. Profiles that showed a marked near surface thermocline coincide with the lowest gradients registered between 1 and 3 m thermistors. On October 4 and 6 a thermocline at 8 m depth could be observed and some individual profiles of the other days showed weak step changes in temperature. The profiles showed the inadequacy of defining a thermocline by a decrease of 0.8^{o}C below the sea surface temperature (Fiedler,

2010). In summary, data from thermistors did not show significant differences between gradient 1-3 m to the gradient 3-5 m as would be expected if a thermocline would be present above 5 m; instead we typically observed a continuous thermal gradient for 1 to 5 m in most CTD profiles.

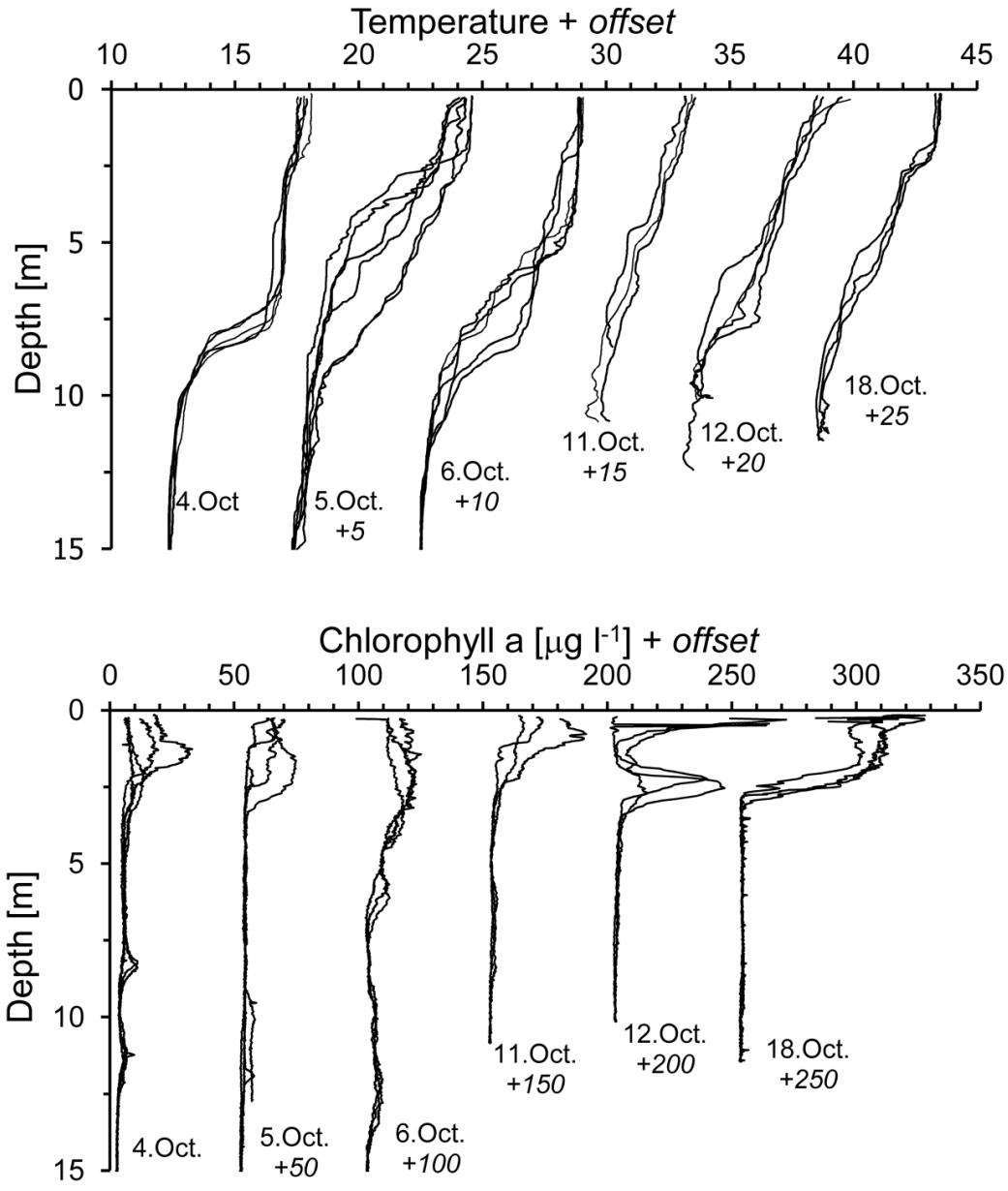

Figure 9 Temperature profiles (A) and chlorophyll profiles (B). CTD profiles on October 4, 5, 6, 11, 12, and 18, 2011 during a dense algal bloom in Todos Santo Bay, Mexico. Profiles of the different days are offset as indicated at the bottom below the dates.

3.1.2 NSTS at ADCP station

For the ADCP station on September 22, 29 and 30, we observed superficial temperature gradients mainly in the first meters with a marked superficial thermocline on September 23 at about 5m, on Sept.29 at about 6m and on September 30 a continuous temperature decline below 3 m depth (Figure 10).

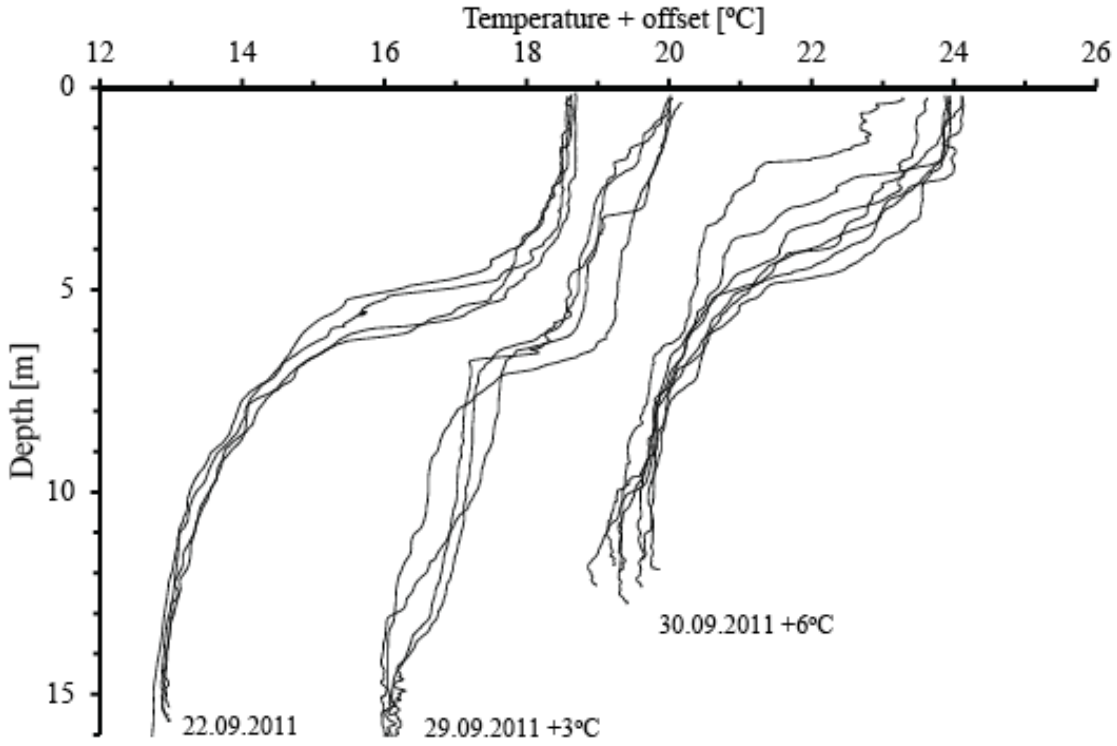

Figure 10 Temperature profiles. CTD on September 22, 29 and 30, 2011 in ADCP station (31º 50.822 N, 116o 41.432 W). Profiles of the different days are offset as indicated at the bottom near the dates.

3.1.3 NSTS at FLUCAR station

At the FLUCAR site we observed in the top 1.5m a homogenous layer and below different stratification types: on September 02 a step change of 1.5^{o}C centered around 2 m, Sept. 22 a minor stratification with step change at 4.5m September 29 a continuous gradient of 3 degrees between 2 and 8m. The temperature stratification pattern for FLUCAR station was varied but all showed significant stratification above 5m depth. (Figure 11).

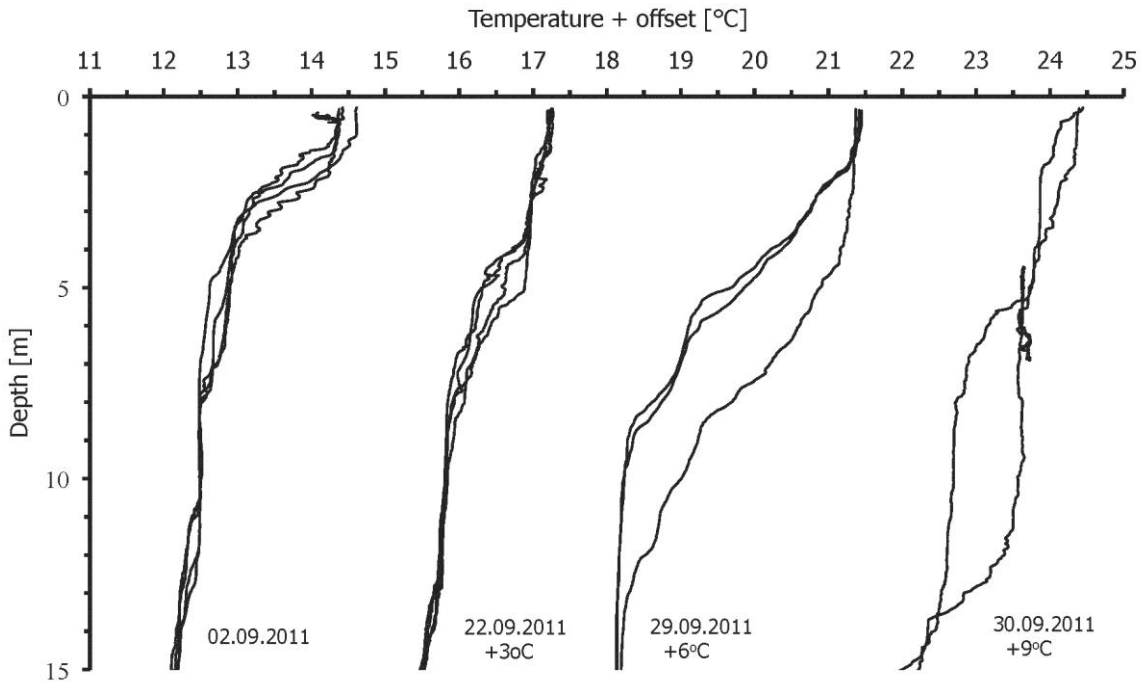

Figure 11 Temperature profiles. CTD on September 22, 29 and 30, 2011 in FLUCAR station (31º 40.25 N, 116o 41.60 W). Profiles of the different days are offset as indicated at the bottom below the dates.

3.2 The surface bloom wind drift (SBWD) transport

3.2.1 Vertical distribution of the bloom forming organism

In situ fluorescence profiles were used to document the presence of the bloom forming organisms within the NSTS. Highest values of chlorophyll concentration were found on October 12 and 18, 2011 (Figure 9B). On October 12 the concentration was 138 mg m^{-2} integrated from 0 to 3 m. On October 4, 5, 6 and 11 the chlorophyll concentration reached 88 mg m^{-2} between 0 and 3 m. In summary, chlorophyll profiles during the sampling period showed a heterogenous distribution and cells were concentrated within a superficial thin layer on October 12, 2011.

3.2.2 Superficial water transport

Surface coastal circulation can be followed by tracking the position of drifters which are expected to stay in the same parcel of water, however additional external forces can act on the drifters such as wind resistance on the surface buoy or currents acting on the cable suspending the drogue. CODE drifters with drogue bodies close to the surface can be affected by the water motion induced by surface waves, thus changing the direction and speed of the drifter from the net horizontal transport. We found good agreement between Holey Sock and Code type drifters in both velocities (R^2=0.78627, $p>0.05$) and bearings (R^2=0.9162, $p>0.05$), adding confidence into the performance of Code-type drifters (Figure 12).

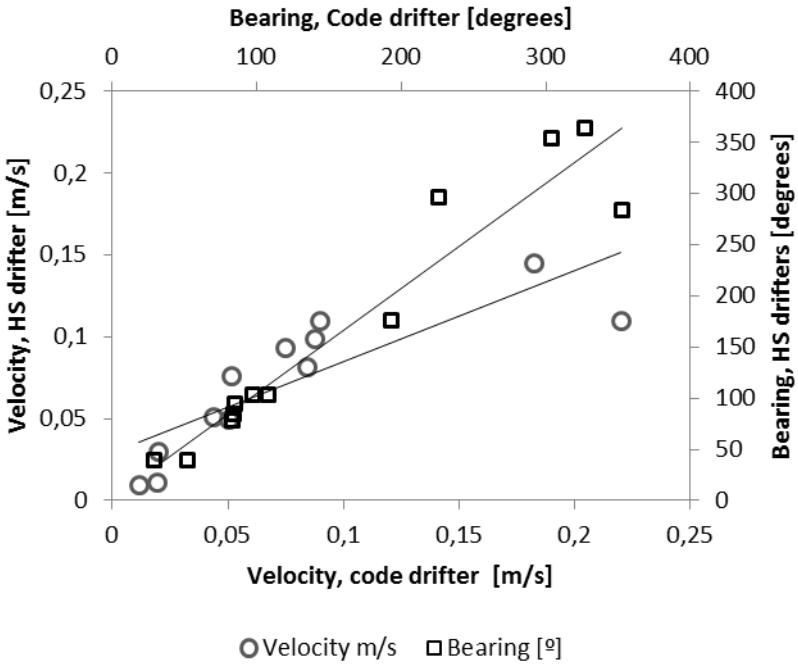

Figure 12 Code type and Holey sock velocity (squares, R^2=0.9161) and bearing (circles, R^2=0.7027) comparison

We also validated the CODE drifters' with an ADCP, finding on September 21, 28 and 29 (2011) similar trajectories and velocities as the trajectories and velocities of 1, 3 and 5 meters CODE drifter's. During the three days, ADCP trajectories showed a spiral current vector distribution with depth where the surface current followed approximately the wind direction and deeper current vectors represented local hydrographic patterns (Figure 13). The similarity in surface current and wind is the result of the uncoupling of the water layer close to the surface from the deeper water currents made possible by the near surface stratification. In general, data obtained from these comparisons suggest that drifter-derived velocities (Lagrangian velocity) do agree with the velocities measured by the ADCP (Eulerian velocity). During ADCP deployments, the wind was directed to 110 degrees with average wind velocities of 0.33 m s^{-1} for the three days of ADCP deployments,

which is lower than the mean wind velocity registered during midday in October 2011 (approximately 5 m s^{-1}) (Figure 14).

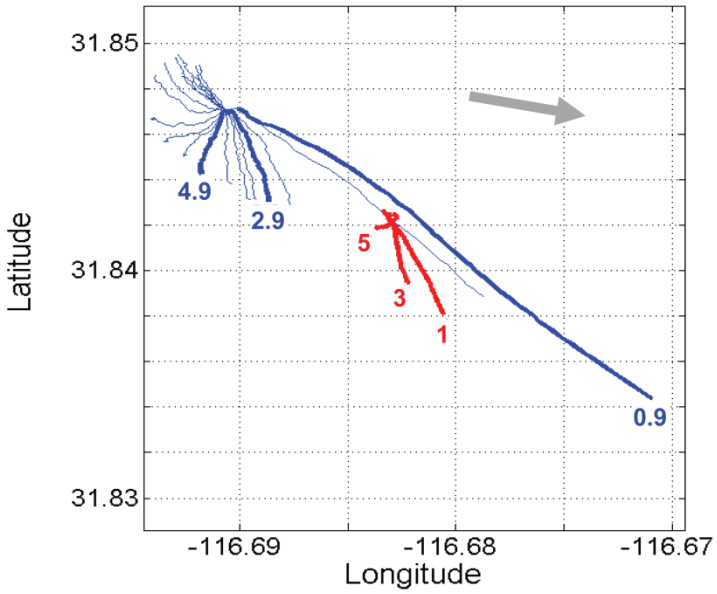

Figure 13 Virtual displacement from ADCP (Aquadopp, Nortek) at 4.9, 2.9 and 0.9 m, and CODE type drifter's trajectories at 5, 3, and 1 m on September 21, 2011. ADCP trajectories are for each 0.5 m. The grey arrow indicates the dominant wind direction.

3.2.3 Wind driven transport.

Monthly wind pattern on October, 2011 showed a diurnal breeze pattern with increasing velocities (Figure 14A) and wind directed toward the coast between 9 and 17 hrs (Figure 14B), resulting in eight hours of thermal breeze, with an average of 5±2 m s^{-1} at midday. We compared the period with the highest velocities between 13 to 15 hrs with the trajectories of 1 and 5 meters drifters (Figure 15). In general, the wind speed measured during the period of 13 to 15 hrs, were from 1 to 6 m s^{-1} and wind direction was directed toward the coast (Figure 15); drifters were transported at speed of up to 0.05 m s^{-1} during the sampling

dates (Figure 16). The 1 m drifter directions were toward the coast except for October 18th, these drifter trajectories were obtained from Holey sock drifter data. The 5m drifters showed a direction very different from the 1m drifters mostly away from the coast and showed velocities between 0.004 and 0.07 m s^{-1}, generally smaller than 1 m drifters. The time course of wind and surface drifter vectors showed oscillations with periods of approximately 20 min. These oscillations are probably the result of Seiches within the bay and the period corresponds to the approximate dimensions of the bay with a depth of 20 m and a diameter of 10 km. Drifter trajectory directions showed a generalized pattern with the 1 m drifter always more directed towards the coast, and the 3 m drifter direction between the 1 and 5 m drifters. Figure 17 shows the trajectories registered for all sampling days during the bloom; on October 4, 5 and 6; the differences between 1 m and 5 m drifter are evident. Although on October 11 and 12 the trajectories of 1 m drifters were also directed toward the coast, 5 m drifters did not show the same patterns as before, instead similar trajectories between 1 and 5 m drifters were found. On October 12 drifters showed a change in direction during deployment that could result from a delayed response to wind-forcing or from tidal currents.

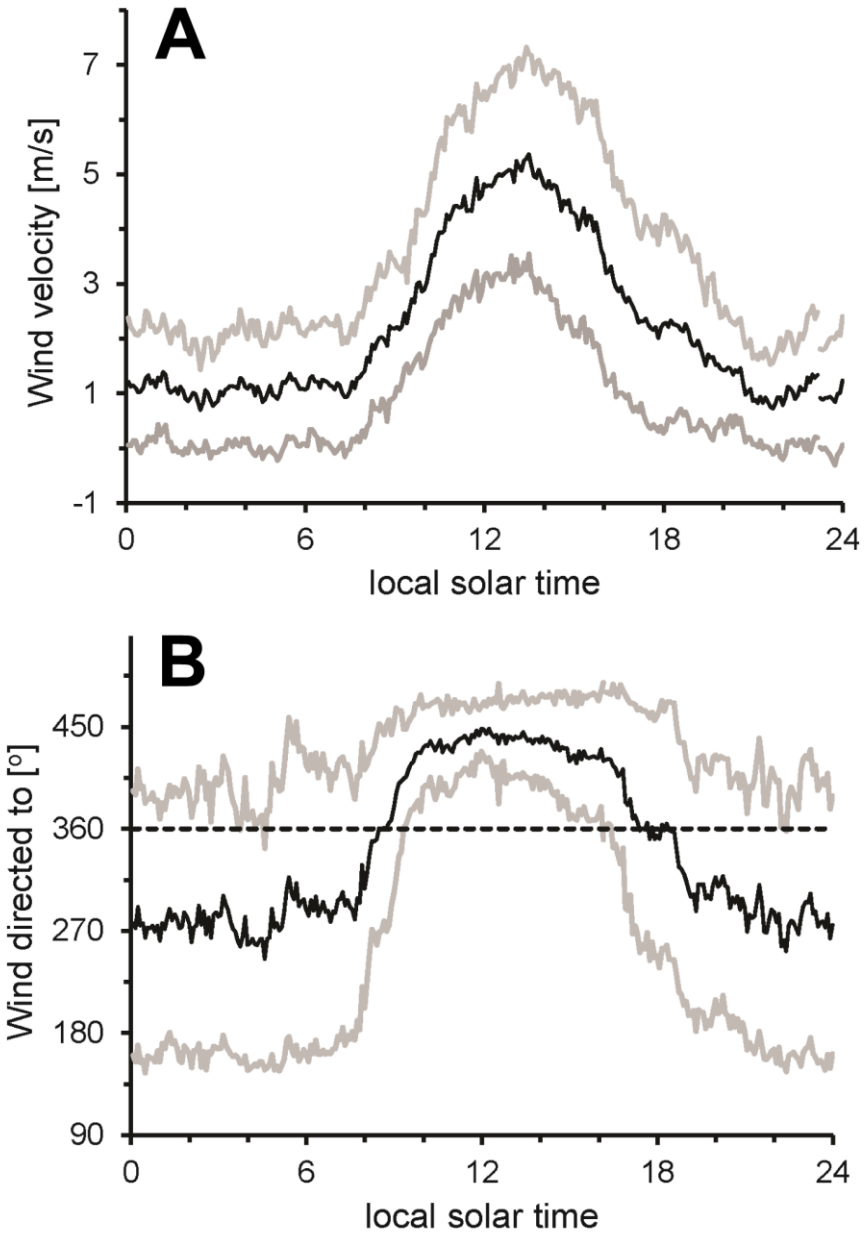

Figure 14 Wind pattern during October 2011. Averages values (black) ± standard deviation (grey). 12:00 of local solar time represent the time of minimum zenith angle. (A) Wind direction and (B) Wind speed.The wind direction above 360 degress was calculated by the measured wind direction plus 360 degres to avoid a break in the trace.

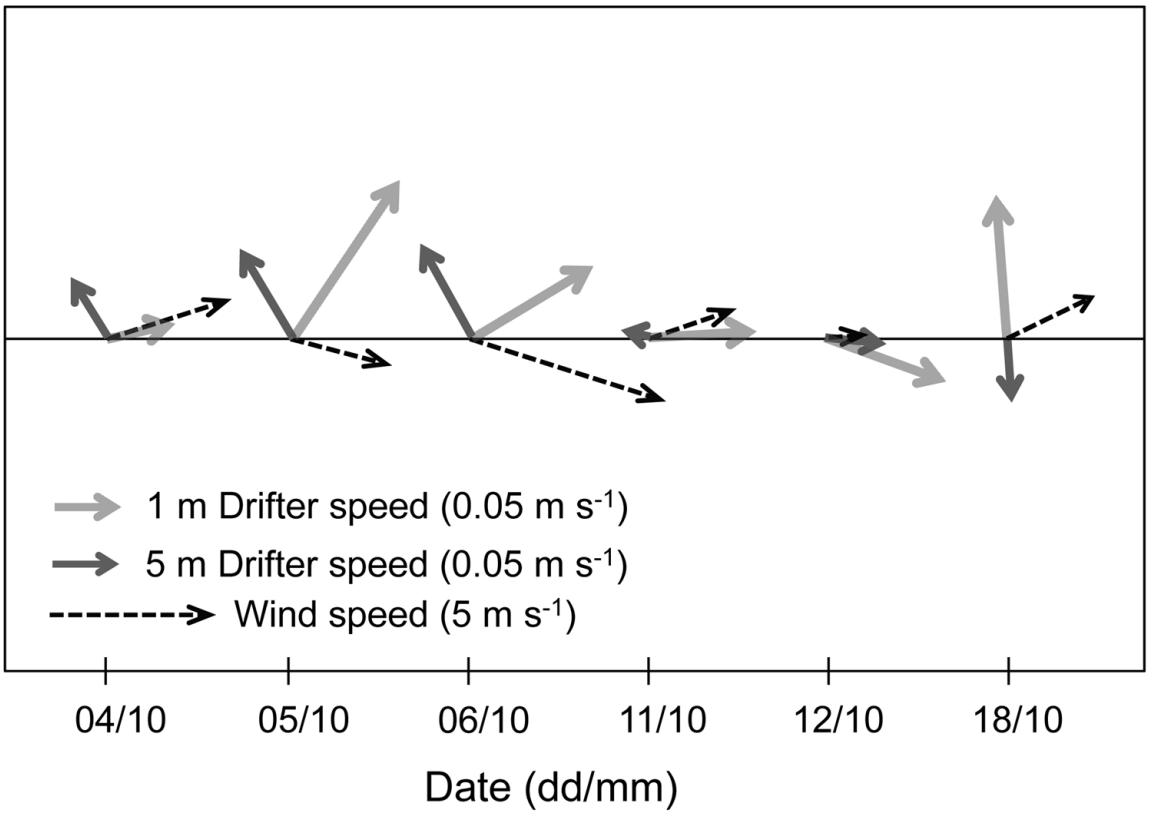

Figure 15 Wind and drifters pattern during October 2011. Averages are from 13 to 15 hrs on October 4, 5, 6, 11, 12 and 18, 2011. Drifter velocities (1m, light gray; 5m, dark) differ in scale from wind velocities (broken black). North is in the ordinate direction and East in the abscissa.

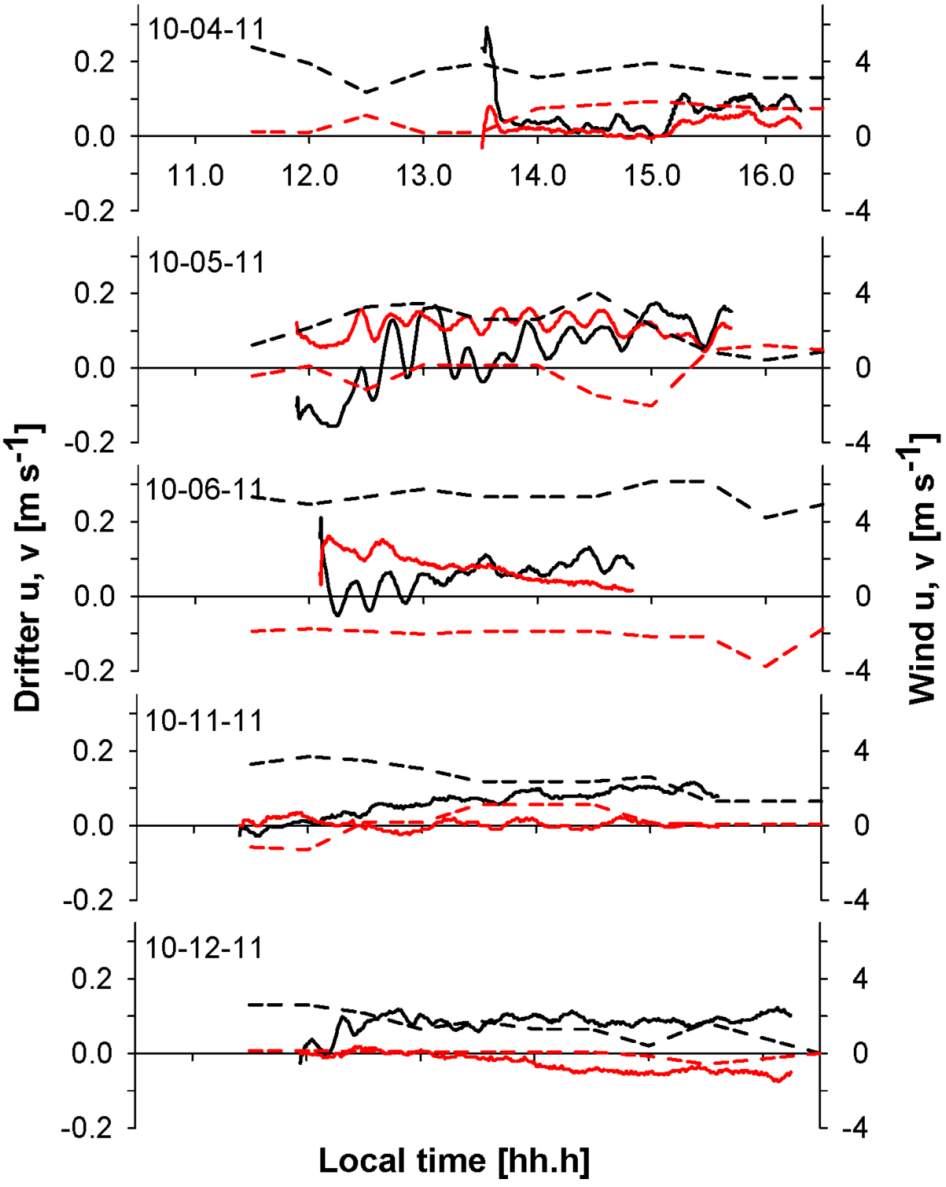

Figure 16 1m drifter and wind velocity components. Time series of the Longitudinal (u) and (v) components, with scales as indicated on ordinates. Wind (dashed lines), drifters (solid lines), longitudinal u (black), latitudinal v (red).

Figure 17 1 m (red), 3 m (green) and 5 m (yellow) drifter trajectories on October 4, 5, 6, 11, 12 and 18, 2011 during a dense algal bloom of *Lingulodinium polyedrum.* Drifters initial position was located within bloom patches.

We estimated the distance traveled by surface buoys during the eight hours of thermal breeze for each sampling day; superficial water parcel traveled on average 2.7 km each day. On October 4, 5 and 6 superficial drifters moved 794, 1058, and 1190 m in 2.8, 3.45, and 2.75 hours respectively. On the second week of the sampling for October 11 and 12 the drifters moved 675 and 1264 m in 2.75 and 3.45 hours respectively. On October 18, the GPS attached on the 1 m drifter turned off during the sampling, so we could not calculate the transport (Table 1).

Table 1. **1 m drifter trajectories during the bloom, distance traveled during deployment with 8 hrs of active sea breeze.**

Date dd:mm:aa	**Logged [m/hrs]**	**Coastward/day [km/8hrs]**
04-10-11	794/2.8	2.67
05-10-11	1058/3.45	2.45
06-10-11	1190/2.75	3.47
11-10-11	675/2.745	1.97
12-10-11	1264/3.45	2.93
Average		**2.7**

In summary, we found a consistent transport of superficial waters toward the coast during the active sea breeze period, and 1 and 5 m drifters showed differences in their trajectories as expected. This persistent transport of superficial waters that contains the bloom forming organisms promoted by the wind is what we called surface wind drift transport.

3.3 *Lingulodinium polyedrum* cells in sediment traps

Mostly vegetative cells were found in the traps, they could be identified by their red chlorophyll autofluorescence and by their cell shape in epifluorescence microscopy (Figure 6A). In cycsts the green auto-fluorecence (GAF) excited by blue or UV light increases in intensity with time after cell death or fixation (Tang and Dobbs, 2007). GAF helped to discrimate cysts from vegetative cells (Figure 6B). We present cell abundance found inside the traps for each day of deployement comparing the proportion of trapped cells with the integrated biomass present in

the surface layer (0 to 3 m) on the day and location the traps were deployed. The integrated biomass was calculated from mg chlorophyll m^{-3} integrated from 0 to the depth limit given in Table II, resulting on October 5, 11 and 18 in an integrated chlorophyll of 88, 55 and 138 [mg m^{-2}] respectively. Recalculating this amount of chlorophyll using the empirical relation (see above) the surface layer from 0 to 3m represented respectively 5.15, 3.15, and 8.19 x 10^9 cells m^{-2}. In the traps we found on October 5, 11, 18, 1.28 x 10^8, 6.47 x 10^7 and 1.81 x 10^8 cell m^{-2} respectvely. For the three days of sediment trap deployment we found an average of 2.3% of the surface layer population reached by the sediment during the following night (Table 2).

Table 2. **Cells reaching the seafloor by vertical migration collected in sediment traps during night. Surface bloom biomass is the integral from the surface to the 'lower depth limit' and given in cells per area and in percentage of surface bloom biomass.**

Sediment deployments dates	**Lower depth limit [m]**	**Chlorophyll integrated 0-3 m [mg m^{-2}]**	**Cells integrated 0-3 m [cell m^{-2}]**	**Cells collected [cell m^{-2}]**	**% surface bloom**
18/10/2011	2.8	138	8.19E+09	1.81E+08	2.21
11/10/11	2.98	55	3.15E+09	6.47E+07	2.05
5/10/11	3.3	88	5.15E+09	1.28E+08	2.49
				Average	2.25

4. **Discussion**

4.1 Importance of the NSTS on superficial water transport

Surface blooms in coastal waters have socioeconomic impacts reaching from respiratory health issues to aquaculture commerce and tourist perceptions (Kirpatrick et al 2006; Pierce et al 2011). Assuming that near surface thermal stratification is a common occurrence; the transport mechanism discussed here may help explain surface bloom dynamics in many parts of the world where sea breezes are commonly present (Hyder et al 2011). Unfortunately few trustworthy data on near surface stratification exist because when common profiling instruments are deployed next to research platforms the data would be subject to a likely but unknown mixing effect. Near surface stratification has been shown in Mexican Pacific waters using specialized instrumentation (Ward and Wanninkhof, 2004; Maske et al 2012), and studied by shipboard radiometric measurements coupled with a physics-based model of near-surface warming (Gentemann et al 2009). By contrast, there is extensive literature on the interpretation of sea surface temperature (SST) because of the possibility of remote sensing, but SST probably has a different dynamic from NSTS. The diurnal SST cycle with cooling during the night has been observed and related to the near surface stratification but more in situ information on near surface stratification is lacking (Donlon et al 2002; Ward, 2006; Minnett et al 2011). The data in this thesis are probably the first to relate measured near surface stratification and wind-driven transport of the surface layer.

Our initial hypothesis considered that the high daylight attenuation in surface blooms would help the formation of the NSTS, however we could not observe any bloom-related surface layer heating, which suggests that NSTS is independent of the presence of surface blooms. An increased heat retention in the surface layer was expected as a result of visible day light attenuation in surface blooms. Approximately half of daylight energy is contained in the infrared radiation (IRR)

and is being absorbed within the first centimeters below the surface independent of the phytoplankton concentration. In blooms the near IRR (<1000nm) reflectance is slightly higher and therefore IR absorption slightly reduced because of high particle back-scattering at the surface but we consider this of minor importance to the near surface temperature budget (Ruddick et al 2006). In blooms the visible light is highly attenuated near the surface; the PAR profiles of the free-rising CTD obtained within the high chlorophyll patches showed very high PAR attenuation, PAR levels at 2 m depth were between 1 and 10 percent of surface PAR when the profiles were extrapolated to 0 meters depth (data not shown). Despite this high attenuation of PAR near the surface, *in situ* temperature measurements during periods of high PAR levels showed no evidence of increased heating of surface waters within blooms when surface temperatures inside and outside bloom patches were compared.

Generally NSTS took the shape of a continuous gradient and typically showed no marked discontinuity that would indicate a homogenous near surface layer. This is contrary to our initial concept (Figure 1), since we hypothesized the formation of a diurnal near surface thermocline with a thin homogeneous surface layer. The NSTS reported here showed no change in stratification pattern during the sampling period, but we sampled only during the day when blooms could be observed at the surface, and therefore we have no information on possible diurnal patters as described before (Gentemann et al 2003). Data from FLUCAR station without bloom conditions also showed a NSTS, confirming that the presence of the NSTS in principle does not depend on high chlorophyll concentration. The presence of a consistent thermal structure in the first 2.8 meters of the water column during a dense algal bloom, (averaging 80 mg m^{-3} chlorophyl)l, led to the question if high concentration of pigments near the sea surface help in the temperature stratification which might result in differences in thermal stratification inside and outside the bloom patches. This surface algae bloom enhanced temperature stratification (SABE-T-Strat) mechanism would indirectly promote the

transport of bloom patches towards the coast by thermal wind. Temperature profiles inside and outside of the blooms showed differences in the upper 2.5 m; however, temperature gradients showed similarities inside and outside bloom patches (Figure 18). Temperature differences are not simple to explain because the heat balance is strongly influenced by meteorological conditions with heat loss processes from the water to the air, such as the heat loss by evaporation and by conductance of sensible heat (Hartmann, 1994). Future analysis of the heat balance will have to include models (Gentemann et al 2009) to evaluate temperature variations in surface waters and predict the vertical temperature profiles within the diurnal behavior.

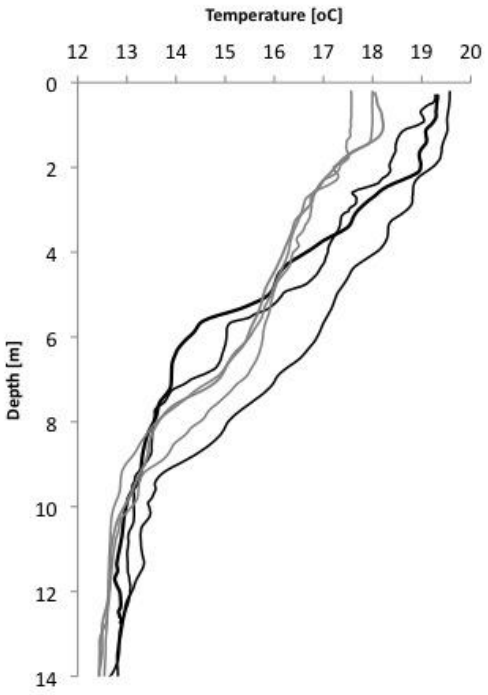

Figure 18. Temperature profiles from CTD on October 5, 2011. Profiles inside a bloom patch (black) and profiles outside a bloom patch (grey) during a dense algal bloom in Todos Santo Bay, Mexico.

The wind stress at the sea surface imposes a boundary condition; the stress at the top. Here we are only concerned with the tangential, horizontal, stress. The depth variation of the stress must be balanced by other terms in the equations of motions, usually producing a sheared flow with magnitude and direction changes with depth. The expected stress and velocity amplitudes at large depths are, in comparison with the surface, insignificant. The common observed shear results in a spiral hodograph with turn in either direction depending on the azimuth relation of surface and deeper water current. The shear flow spiral is present in the ADCP data taken from 10m upwards before the bloom period (Figure 10). The drifter trajectories before and during the bloom are also consistent with a spiral pattern as proposed in Figure 10. Since this flow spiral responds on short time scales to varying winds, it bears no resemblance to Ekman-like spirals which are steady end conditions. In contrast to the Ekman spiral the shear flow under varying wind can turn either way, and even with no velocity attenuation with depth (Price et al 1987).

In the vicinity of 30° latitude, diurnal breezes are near resonant with inertial waves, which, even with the lack of lateral freedom imposed by the coast, and topography generate relatively large, daily-oscillating ocean movements. It has been proposed that these daily oscillations favor nutrient supply towards the surface and the coast (Hyder et al 2011; Lucas et al 2012). For the purpose of ecology bloom transport, we consider here only the onshore transport due to wind (Figure 11A and 11B). The relationship between wind pattern and water movement is observed in Figure 8, wind data indicate onshore trajectories with maximum velocities of 5.1 m s^{-1}, a typical wind velocity reported for this location (Hernandez-Walls, 1986). During the day the strong winds associated with the daily sea breeze can produce onshore surface currents at 1 m depth with velocities of up to 0.01 m s^{-1} similar to the 0.01 to 0.015 m s^{-1} found near our site during summer conditions (Álvarez-Sánchez et al 1988; Tapia et al 2004).

The general pattern, of drifter trajectories for all days, showed differences between surface (i.e. 1m drogue) and 5m drogue drifter trajectories (Figure 13). On October 5, 6 and 18, surface drifters did not have the same direction as the wind, which probably resulted from an interaction between wind and current forcing. A similar has been observed during a tracer transport experiment related to transport of larvae (Kaplan et al 2005; Tapia et al 2004). During October 5 and 6 (Figure 9) we observed velocity oscillations in with periods of approximately 20 min (Figure 19) which are probably due to Seiches. In Figure 20 after removal of the velocity trend, the velocity oscillations are shown to be oriented across the bay, as expected for Seiches. These oscillations have no significant effect on the overall transport of the water but might well affect the ecology of the benthos including the sedimented cysts. Semi-enclosed systems are susceptible to these natural oscillatory motions. Resonance at these sites generates strong currents that resuspend sediments and other particulate material from the seafloor (Jordi et al 2008). In the ocean, Seiches are most significant in confined areas, and can contribute to the dynamics of near shore algal blooms (Anglés et al 2010).

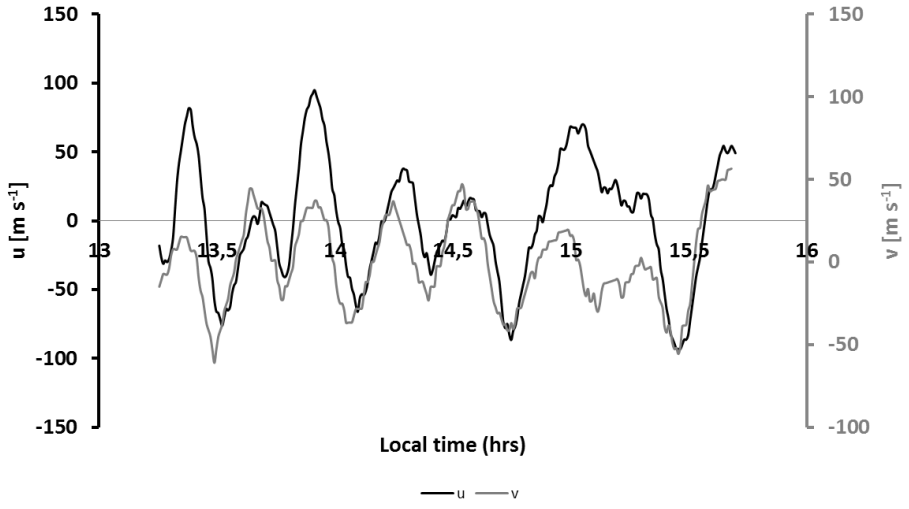

Figure 19 **u and v components of 1m drifters on October 5, 2011. A 20 minute period oscillation in both directional components can be identified.**

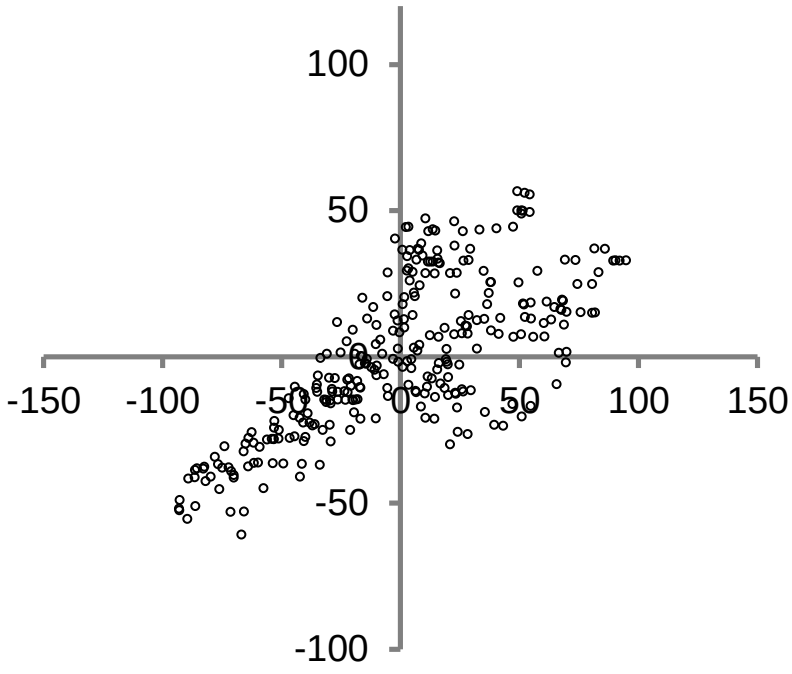

Figure 20 Current direction of the current anomalies observed on October 5, 2011.

4.2 Ecological implications of the SBWD

The combination of diel vertical migration and diurnal onshore transport facilitates the maintenance of bloom forming organisms. Surface bloom forming dinoflagellates show a typical diel migration pattern that allows the population to obtain nutrients during night and photosynthesize during the day at the surface (Cullen, 1985; Dortch and Maske, 1982; Cullen and MacIntyre, 1998). When sufficient nutrients are available at the surface, the dinoflagellates show reduced vertical migration tendencies (Cullen and Horrigan, 1981). Vertical migration also provides *L. polyedrum* at night with a less turbulent environment during the time of cell division, potentially beneficial for *L. polyedrum* because of its sensitivity to shear flow during cell division (Juhl and Latz, 2002). Arguments linking nutrient

limitation and vertical migration have considered inorganic nutrients but not vitamins. *L. polyedrum* is vitamin B12 auxotroph (Tang et al 2010), maybe the benthic bacteria provide them with the necessary vitamin B12 for population growth? There are still many ecophysiological aspects of bloom development unknown. Here we argue that the shoreward transport of the bloom helps to maintain the bloom and increases the possible redevelopment of the bloom in the future, considering the arguments provided by the literature: Bloom organisms reaching the sediment would have more nutrients available (Sinclair and Kamykowski, 2008), avoid horizontally dispersion during the night (Yamamoto and Okai, 2000), and have a potentially shallower seedbeds for the initiation of future blooms (Pena-Manjarrez et al 2005; Tobin et al 2011).

We found high cell densities of *L. polyedrum* in near surface thin layers (Figure 5, 12-oct-2011). Different mechanisms forming thin layers have been proposed, from physical processes, such as the interaction between vertical shear gradients and vertical migration (Franks 1992), the horizontal advection of phytoplankton patches to physiological adaptations that increase the net growth rate (Donaghay and Osborn, 1997; Dekshenieks et al 2001; McManus and Woodson, 2012; Cheriton et al 2009; Omand et al 2011). We propose an additional mechanism based on the shear flow spiral and the patchy horizontal distribution of the bloom: The spiral shows current vectors of small vertical distance with significantly different azimuth directions (Figure 15). A bloom patch that is vertically homogenous over the top 3 meter can be transported in different directions and a deeper layer can be transported into a region with no bloom at the surface. This transport could lead to the observed thin layer (Figure 6B, 12-oct-2011) but it could also help to distribute the bloom patches horizontally and dilute the concentration in bloom patches assuming that the organisms would migrate to vertically redistribute themselves in the surface layer.

We observed a net onshore transport of blooms of approximately 2.7 km day^{-1} calculated from the average drifter velocity and the period of coastwise sea breeze. A cell with an average generation time of two days (Smayda, 1997) would be transported 5.4 km onshore before cell division. This distance should be significant considering that extensive *L. polyedrum* blooms have been observed near the coast of California typically at a distance ranging from ~500 m from shore (Omand et al 2011) to around 20 km for example: near our coast during a dense algal bloom in 2005. The onshore movement becomes important because it coincides with nutrient gradients perpendicular to the coast over this distance. Also the sea floor depth will be shallower making it easier to be reached during down migration.

Our sediment trap placed below high concentration surface patches and collected during one night trapped about three percent of the vegetative cells in the bloom surface population and a low number of cysts. The percentage of migrating vegetative cells (Table 2) can be considered the minimum percentage because we normalized using the high concentration within the surface bloom patch, but maybe a better reference would be the average concentration in the bay because during the hours of downward migration the horizontal water movement could mix the surface source population, therefore part of the trapped population probably originates from a lower chlorophyll concentration surface layer. We estimated the percentage of migrating cells by considering the average of cells during the sampling (inside + outside patches), resulting in 6% about twice the percentage calculated using the surface bloom cell concentration.

In terms of the bloom cover in the study area, we consider that based on visual observation about 1/3 of the area is covered with the patches of the bloom forming organism, and 3/4 of the bloom population is the surface population. To get a more quantitative estimate of bloom coverage we tried to document the area of bloom coverage within the bay with digital images using a digital camera with

polaroid filter from a hill (400 m) located in the southern part of the bay and in the highest building of CICESE (Supplemental information). We expected that the geo-referenced images would allow us to quantify the horizontal movement of the patches and with contrast enhancement analysis we would quantify the coverage of the bloom; however, we were not able to process the trichromatic images and increase the bloom contrast sufficiently to identify the bloom patch extension.

The interpretation of vertical distribution and migration was not straightforward; during the days of sediment deployments (October 5 and 11, 2011) chlorophyll profiles outside the patches also showed two maximum, one at 3 m and a second one at 8 m that coincide with the expected mixed layer, unfortunately we do not have the cell concentration of this second maximum because we only collected water form 1, 3 and 5 m. For further interpretation of cell migration we need to consider the possibility of different bloom forming populations. Even though we did not sample below 5 m, Lewis et al 2012 reported that before the *Lingulodinium polyedrum* bloom started at the end of September 2011, a sub-superficial (10 m) bloom of *Pseudonitzchia* was present. The presence of two different bloom forming organism within the water column would complicate the interpretation of migration patterns.

Besides the results discussed above, the importance of the surface water wind drift on the maintenance of dense algal bloom is based on the swimming behavior of dinoflagellates. Considering a maximum swimming speed of 278 $\mu m\ s^{-1}$ for *L. polyedrum* (Smayda, 2010) the surface population can reach 12 m depth within 12 hours, a depth close to the deployment depth of the traps. These deep migrating cells might not migrate to the surface the same day. Cysts can reach the sediment by sinking passively through the water column during the night. Cysts that reach the sediment at a shallower depth could presumably return to the vegetative state and start a new bloom under more favorable conditions. The relationship between the cell cycle and diurnal vertical migration has been

recognized as an important part of bloom dynamics (Katano et al 2011) however, swimming behavior may vary among dinoflagellate species (Ji and Franks, 2007) and under different environmental conditions such as temperature stratification, light (Kamykowski and Zentara, 1977; Heaney and Eppley, 1981) and nutrient limitation (Kamykowski and Yamazaki, 1997; MacIntyre et al 1997; Doblin et al 2006). In either case, a more shallow water environment will be beneficial to grow, divide, or leave the cysts for the next bloom.

5. Conclusions

In this research, we demonstrated the presence of near surface stratification that is promoting the wind drift of the surface layer. We showed how this wind drift could transport surface blooms closer to the coast and we suggest that this mechanism is helping the organisms to maintain the bloom. We documented a consistent near surface temperature stratification during a dense algal bloom that is also present in non-bloom conditions. During eight hours of active thermal breezes typical for upwelling areas the physical feature with all the surface layer constituents was easily transported toward the coast about 2.7 km. We lack the data to demonstrate a diurnal behavior of near surface temperature. We found a low percentage of surface bloom cells migrating toward the sediment: this low percentage would increase if we consider the average surface cell concentration instead of considering only the high surface bloom concentration. A further consideration for the interpretation of the migrating pattern is to give more attention to the composition of the different thin layers that might be found during a bloom.

The transport mechanism discussed and documented here for near surface waters, will not only transport blooms, but all dissolved and particulate constituents of the surface water; some of these constituents could be larvae, or contaminants released near the coast with ship ballast water or from waste water outflows. This

coast-wise transport has been rarely documented in coastal waters and its consequences have been little considered in the literature. Finally, it is important to highlight the importance of relating physical transport with the physiology state of the bloom forming organisms in order to understand the dynamics of dense algal blooms. In this case, future work should include the detailed analysis of the effect of light absorption on the superficial temperature dynamics. Additional work should be focused on the relation between the rates of division of the species involved and how these rates can be compared to hydrographic transport or dispersion. One of the specific objectives in this project was to demonstrate the role of diurnal vertical migration on the maintenance of the bloom due the wind driven transport. An experimental approach was unsuccessfully tried with an artificial water column of 2.5 m length, thus some of the questions that we will try to approach experimentally in the future will be: (1) How is the diurnal vertical migration pattern related with cells division rate and (2) Does the taxonomic composition of the migrating cells resemble the composition of the surface bloom?

CHAPTER II. The Mitotic index for growth estimates of natural populations, challenges and prospects: Methodological approach.

1. Introduction

In biological oceanography the specific growth rate μ (day $^{-1}$) of specific species in mixed populations is necessary to interpret the environmental factors that can control the population dynamics. Historically, there were two models to obtain specific growth rates via cell cycle; the mitotic index method (McDuff and Chisholm, 1982) and frequency of diving cells method (FDC) (Carpenter and Chang, 1988), the basic concept of both methods consist in establishing under controlled conditions a relation between the fraction of cells in division or mitosis and cell division rate. Another way to follow the cell cycle is to quantify the relative DNA content of individual cells; in this case, the percentages of cells in each cell cycle stage are estimated from DNA frequency histograms (Cetta and Anderson, 1990).

The methods mentioned above use flow cytometry (FC) or micro fluorometry to detect each cell cycle stage using the amount of fluorescence as an indicator. The advantage of flow cytometry is the larger numbers of cells that can be analyzed increasing statistics and yielding an increased accuracy of the cell cycle stage determination. Recently, FC has also been used to identify species and life cycle in dinoflagellates by discriminating and quantifying cells on the basis of their nuclear DNA content, and thus distinguish between species and life cycle stage (Figueroa et al, 2010). Although flow cytometry has advantages over other methods to detect the cell cycle stages, it uses expensive instrumentation that is not always available. Also, FC has the drawback in a mixed population that the cells cannot be identified taxonomically. For these reasons we looked for a method to detect the cell cycle stage using wide field microscopy, that would be easier to

apply than previous methods and eventually lending itself to apply to mixed field samples.

Since *Lingulodinium polyedrum* has a U shape nucleus (Alverca et al 2005); we assessed the possibility to use geometric proxies of the U shaped nucleus that can be easily observed in the epifluorescence microscope to estimate the cell cycle state, for example the distance between the two endpoints of the U or the length of the arms. We try to avoid the quantitative estimate of fluorescence intensity as a marker for the cell cycle state because the fluorescence intensity is dependent not only on the quantity of nucleic acid but also on the state of the staining dye and the staining protocol.

At this moment the method development is still in process, here we report the present advances and future challenges.

2. The concept

The cell cycle of eukaryotes consist of four discrete and sequential phases named G1, S (DNA synthesis), G2 (second gap), and M (mitosis). In order to study the cell cycle, it is critical to determine the localization of cells in the different cell cycle phases. The distribution of cell-cycle state of the stained population is then analyzed; the distribution obtained can be deconvolved to identify the different populations G1, S and G2.

The method proposed here is based on detecting changes in dinoflagellates nucleus volume in the different cell cycle stages to estimate division rate, assuming that the volume observed in the microscope is related to the cellular DNA content. During the cell cycle the quantity of cellular DNA increases and with it the volume of the nucleus and therefore the geometry of the nucleus: in G1+ S there will be 1 copy of the genome and in G2+ M will be 2 copies of the genome (Figure 21). The ratio of G1 + S to G2 cells together with the temperature will allow us to estimate the specific growth rate based on the percentage of the cell population that resides in a certain stage of the cell cycle;.

Two models have been used to follow the cell cycle, the Mitotic Index (MI) developed by (McDuff and Chisholm, 1982) and the Terminal Event model (TE) developed by (Carpenter and Chang, 1988). The MI model follows the frequency of dividing cells by microscopy and obtains the growth rates estimations by dividing the amount of cells representing M phase cell cycle stage and the cells in division represented by G2+S+G1 stage or the cells that have 2 copies of DNA. In the TE model, the number of the cells that are in the S+G2+M (2 x DNA) are divided by the cells in G1 (1x DNA). Here we will use the second model, based on the observation that G1 cells will have less DNA fluorescence than S+G2+M. Because the quantitative use of fluorescence is problematic we are suggest using other

proxies that represent the amount of DNA during the cell cycle, for example the nucleus volume.

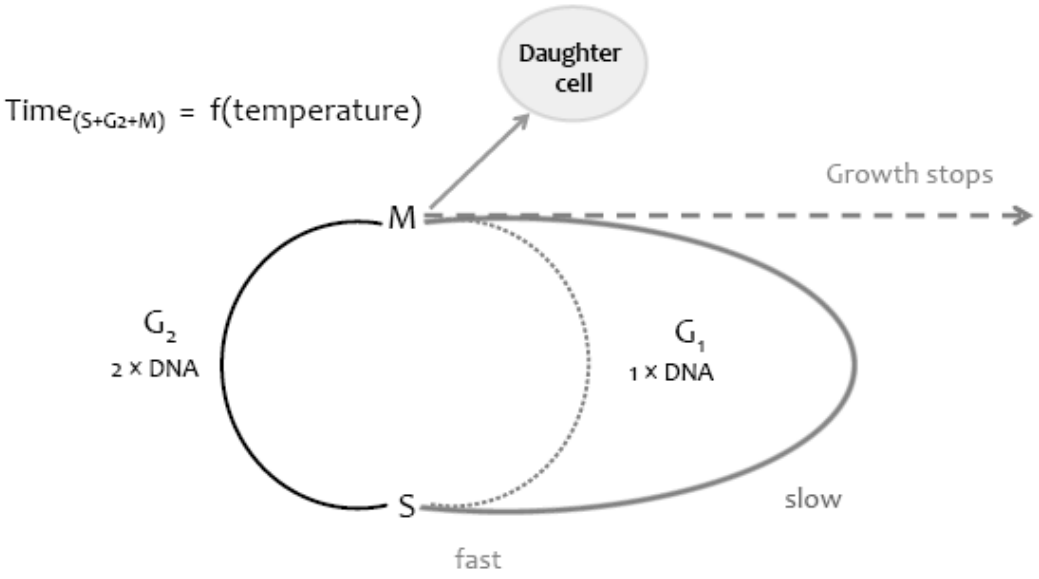

Figure 21. Representation of the basic concept of the cell cycle.

We started with U shaped nucleus of some dinoflagellates as a model (Figure 22 and 23); we consider that the length of the nucleus (L) is constant and the nuclear volume is: $V_{nucleus} = L\pi\left(\frac{D}{2}\right)^2$, where, L is the length of the nucleus and D the diameter of its arms (Figure 22)

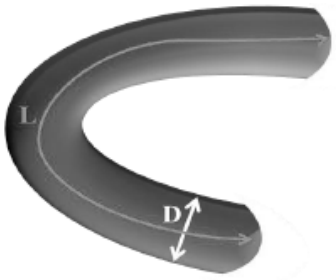

Figure 22 Representation of *Lingulodinium polyedrum* nucleus, its length (L) and diameter (D) are indicated.

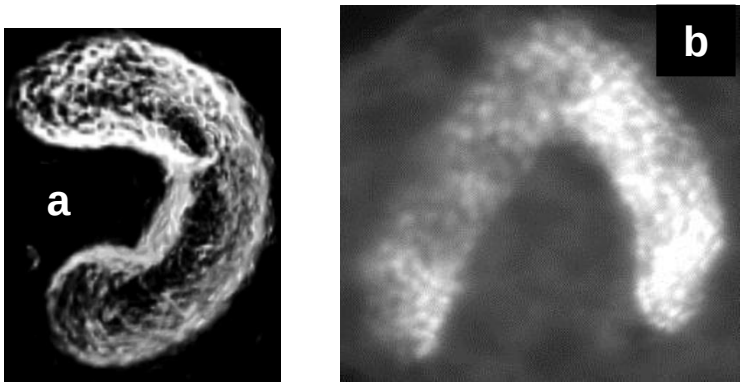

Figure 23 (a) 3D reconstruction of U shape *Lingulodinium polyedrum* nucleus after image analysis. (b) U shape nucleus after stained with DAPI.

3. Methodological advances

3.1 Sample treatment:

Lingulodinium polyedrum HJ acclimated at 20^{o}C and 12:12 L:D cycle in L1 medium

- Fixation with 1% of glutaldehyde for 15 minutes.
- Centrifugation at 800 RPM for 3 minutes to wash cells.
- Remove supernatant

10 ml of *Lingulodinium polyedrum* concentrated cells

- Resuspend cells with 10 ml PBS 1x + DAPI [10 ug ml-1] + Calcofluor (SIGMA) [2ug ml-1]
- Stain for 30 minutes in dark and at 4 ^{o}C
- Centrifugation at 800 RPM for 3 minutes to wash cells
- Remove supernatant

Lingulodinium polyedrum stained and concentrated cells

- Take 10 µl of cells and mount on glass slide
- Select cells in eplifluorescence microscope
- Acquire 3D images stacks

3.2 Microscopy

For epifluorescence micrographs and epifluorescence microscope (Axioskope II plus, Carl Zeis, Oberkochen, Germany), using a fiber optic coupled Xenon lamp and an X100 objective lens (Plan-Appchromat, Carl Zeiss). A dichroic filter DAPI (FT395) was combined with 358 excitation and 460 emission filter. Images were captured with a cooled CCD camera (ANDOR tecnnology, CT, USA), assisted with a Z stack controller, acquired and processed with Micro-Manager open source microscopy software (Edelstein et al 2010). Image analyses were done using the open source software ImageJ v. 1.46 (Rasband, W.S., ImageJ, U. S. National Institutes of Health, Bethesda, Maryland, USA, http://imagej.nih.gov/ij/, 1997-2012).

3.3 Images analysis

3.3.1 Nuclear volume and cell size proxies

The determination of nuclear proxies and relative nuclear volume includes the analysis of digital images taken with a digital camera coupled with an epifluoresence microscope at different focus depth (stacks). The stack was converted to a single image with the maximum pixel values. Once a single image was created, different measures were taken from the image (e.g. length of the arms, the diameter of the final part of the arm, the length of all the nucleus, etc) (Figure 24 and 25).

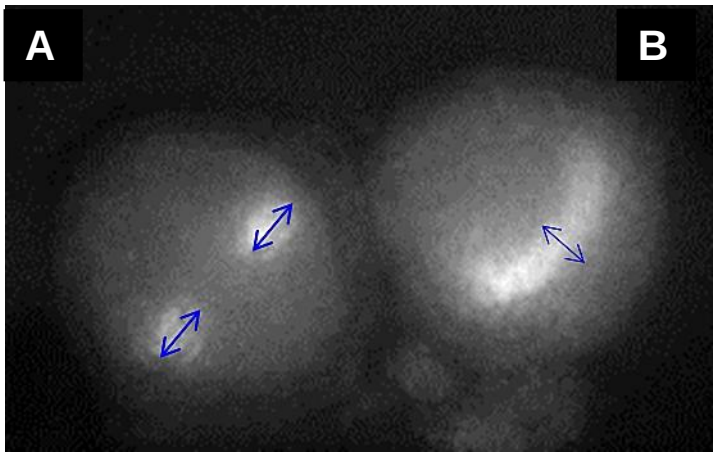

Figure 24. Cells *of Lingulodinium polyedrum* nuclei after staining with DAPI, proxies are indicated with the arrow (a) diameter of the final part of the arm, (b) arm width.

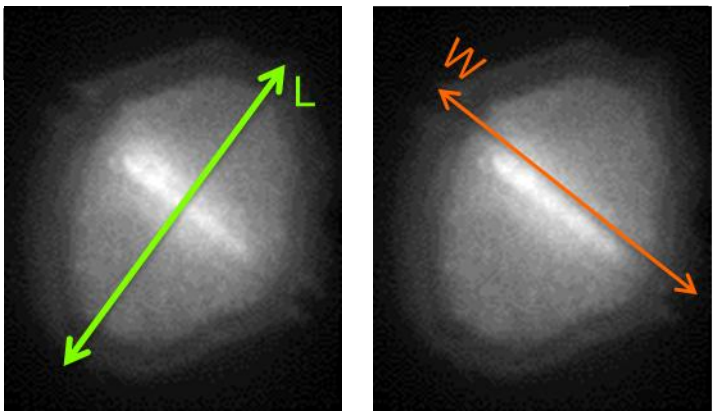

Figure 25 Cell size proxies (L) length of the cell and (W) width of the cell

3.4 Microscopic observations

3.4.1 Comparing different nucleus proxies (thickness of U nucleus, total length and arm length) and cell sizes proxies

We related the geometric property of the nucleus with the phases of the cell cycle over the course of the day. After the comparisons of different proxies to calculate the nuclear volume we found that one important consideration is the orientation of the cell, because it could influence the quantification of the different proxies. Figure 26 shows the different orientation that can be present during the analysis and visualize the difficulties to standardize the measurements of the proxies. At this moment some data suggest that cell size may be a better indicator of the cell cycle stage. In principle nucleus proxies should be less influenced by environmental variables that might change the cell size independent of cell cycle stage. We observed that distribution of the thickness of nucleus proxy changes with time, mainly between 3:00 and 9:00 hrs, when the nucleus arm width changed the cell width was also found to change (Figure 27). We expected that cells with smaller size in the nucleus arm width were the cells after mitosis. Cells at 3:00 am showed the bigger size in the cell width proxy, and after several observations during the monitoring of cell cycle, we found that *L. polyedrum* divided in a period between 3 and 5 am, under transmission light we could observed that cells increase its size.

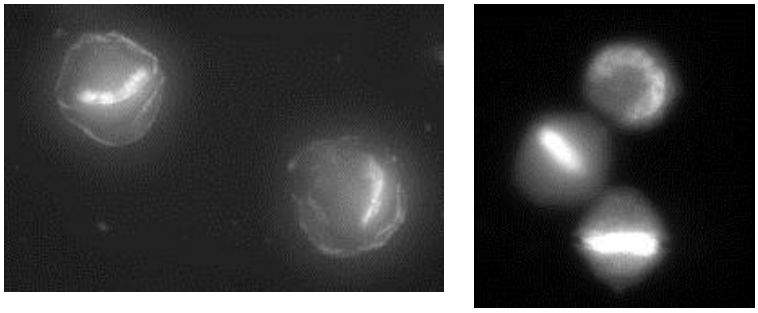

Figure 26 *Lingulodinium polyedrum* cells with stained nucleus showing the different orientation of the nucleus.

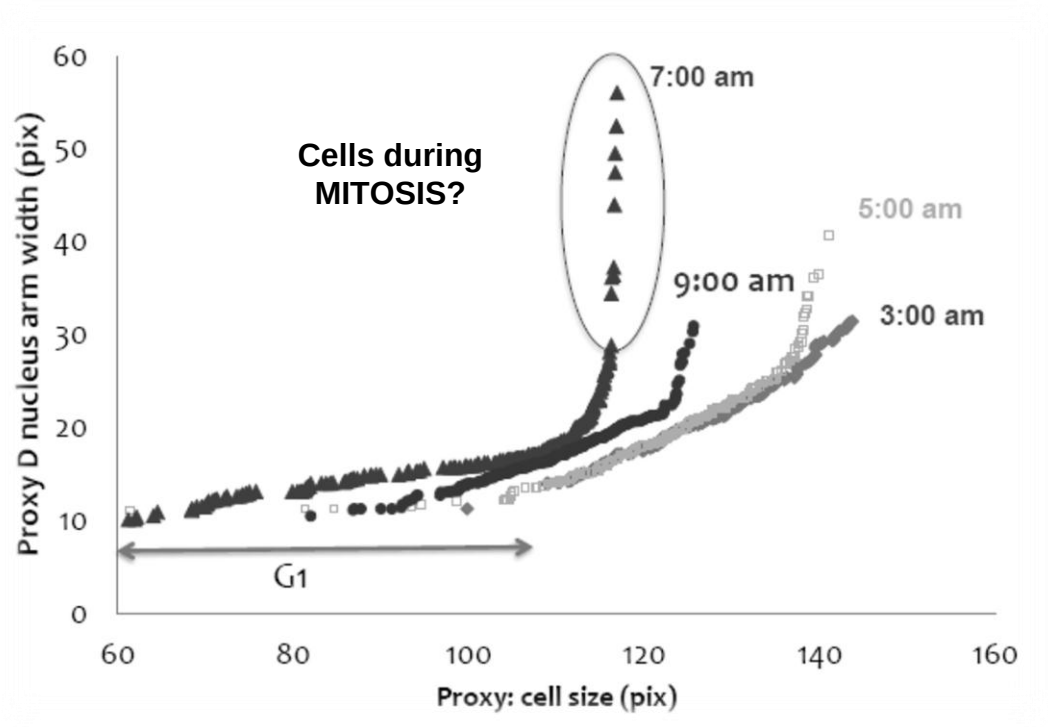

Figure 27 Relation between cell size and nucleus arm width at 3:00, 5:00, 7:00 and 9:00 am.

3.5 Flow cytometry observations

To validate our method it is important to compare the results from image analysis with some standard methodology. Flow cytometry has been used to document and quantify different cell cycle stages in phytoplankton, including *in L. polyedrum* (Dagenais-Bellefeuille et al 2008). For flow cytometry measurements, Sybr green I (Molecular Probes, Eugene, OR, USA) was used to stain DNA-RNA material in *L. polyedrum* cells. Counting and characterization of *L. polyedrum* cell cycle stages were performed using a FACScalibur flow cytometer (Becton Dickinon) equipped with a 15 mW air cooled 488nm argon-ion laser. The FL3 detector (red fluorescence, >650 nm) was used with a threshold allowing only the detection of particles containing chlorophyll, thus assumed to be *Lingulodinium polyedrum* cells. Polygon gates were draw around population, and events falling within these polygons were counted using the software program CellQuest (Becton Dickinson). An epi-fluorescent (Olympus BX51) was used to identify and describe *L. polyedrum* nuclear fluorescence status and cell conditions. The microscope was equipped with a mercury vapor lamp, and an Olympus DP72 camera.

The optimal concentration for these experiments was 0.1 μl^{-1} of Sybrgreen I (dilution 1:10000, from the original stock). After sample concentration, samples were transferred into flow cytometer tubes and stained with the fluorescent DNA-RNA specific dye. Tubes were incubated in the dark at room temperature for 15 minutes before flow cytometric analyses. Sybr Green fluorescent was measured at 515 nm (green, FL1 detector) by flow cytometry. Presence of chlorophyll pigments in *L. polyedrum* was measured at 650 nm (red, FL3 detector). Subpopulations of interest were gated. Fluorescent Beads (Bang labs, 580 nm ex) were used to calibrate the flow cytometer. The beads were diluted 1:1000 to create a working stock that was enumerated. Samples were acquired on the low flow rate setting

(approximately 30 μl min-1) until at least 300 beads and 200 *L. polyedrum* cells were recorded.

3.5.1 Cell staining

During flow cytometer analysis we observed several changes in the stained cells; these changes were related to the Sybr green chromophore stability. Several studies used flow cytometer methods to evaluate changes during the cell cycle, however the majority of them used DAPI (Gisselson et al 1999), Propidium Iodide ((Dagenais-Bellefeuille et al 2008) or YOYO-1 (Jochem and Meyerdierk, 1999) to stain nuclei. These fluorochromes are excited under UV excitation. In our experiments the flow cytometer did not have a UV laser, so we decided to use Sybr green as the flurochorome. It has a strong binding affinity for double-stranded DNA, but it also binds with single stranded DNA and RNA with lower affinities. We used Sybr Green because it is best excited at 495 nm allowing cell cycle studies on more economical flow cytometers. Sybr Green has been tested on marine picoplankton to enumerate cells and for cell cycle analysis of natural populations (Marie et al 1997).

We observed that during sample processing cells stained with Sybr Green increased fluorescence emission with time (Figure 28), complicating the quantification of the flow cytometric data in relation to the cellular DNA content. If the fluorescence changes during the analysis of the sample even the relative frequency distribution of DNA would be difficult to extract from the data. In order to circumvent the change in relative emission the staining procedures and analysis require careful attention. Because Sybr Green is staining RNA it would be advantageous to eliminate RNA fluorescence through the use of RNAase (Nuñez 2001).

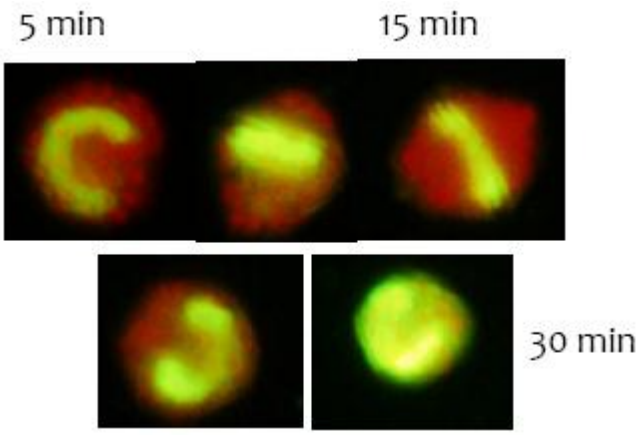

Figure 28 *Lingulodinum* polyedrum cells stained with SYBR green dye (Molecular Probes) after 5, 15 and 30 minutes. Red auto fluorescence is also present. Epifluorescence microscopy with 20x objective.

3.5.2 Cell damage

Besides the problem of cell over-staining, another factor that can affect significantly our cell cycle analysis either with microscopy or flow cytometry, namely the potential cell damaged during the staining procedure. The damage can be the result of the washing procedure and sample concentration protocol, for example centrifugation. We found that cells are frequently damaged at velocities > 800 *g* and centrifugation times > 3 minutes (Figure 29). Haberkorn et al (2011) reported that *Alexandrium minutum* cells are severely damaged upon exposure to thermal, chemical and mechanical stresses, including high-speed and long times centrifugation. We tested different centrifugation times to improve the Sybr Green washing procedure, and the sample concentration. The optimal centrifugation time before cell damage was 800 *g* for 3 minutes for only two cycles.

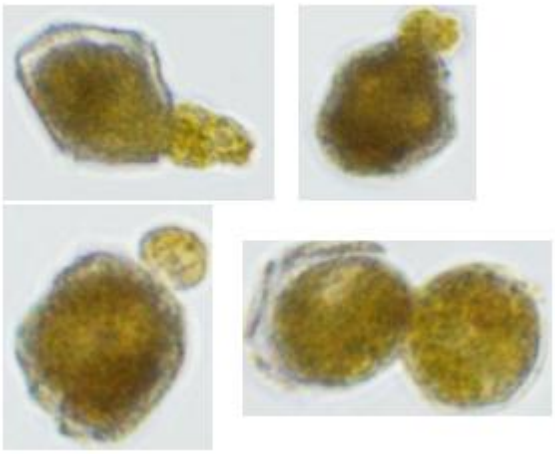

Figure 29 Damage *Lingulodinium polyedrum* cells after high speed centrifugation. Transmission microscopy with 20X objective.

4. Future challenges.

In order to understand the main processes that controls the populations over the time course of a bloom, it is necessary to know the division rate of the natural populations. During the last meeting of The Global Ecology and Oceanography of Harmful Algal Blooms Programme (August, 2012) focused on the advances and challenges for understanding physical-biological interactions in harmful algae blooms (HABs) in stratified environments, the consensus was that at present there is not a universal method to estimate the specific growth rate The lack of an accepted method motivated our search for a robust, reliable and practical method for estimating growth rates in natural populations. The correct estimation of the specific growth rate would allow to investigate in more detail the mechanisms and behavior of the bloom forming organisms, such as distinguishing between physical concentration and dispersion and growth dynamics of certain target species. At present the method is not yet fully developed. We still hope to develop the use of nuclear volume as a proxy of cellular DNA concentration to result in a potentially practical field method. Currently the method still needs to resolve question of stain-

stability and cell damage for flow cytometer and microscopic analysis. It is also necessary to do more tests to have statistical confidence detecting the different stages during the cell cycle; the number of acquired cells is critical in order to ensure a robust analysis. The temperature dependence of the method has to be investigated and finally the method has to be compared with direct estimates of population growth dynamics.

.

6. References

Alvarez-Sánchez LG, Hernández-walls R, Durazo-Arvizu R (1988) Drift patterns of lagrangian tracers in Todos Santos Bay. Ciencias Marinas 14: 135–162.

Alverca E, Franca S, Moreno Díaz de la Espina S (2006) Topology of splicing and snRNP biogénesis in dinoflagellate nuclei. Biology of the cell 98(12):709-720.

Anderson DM, Cembella AD, Hallegraeff GM (2012) Progress in Understanding Harmful Algal Blooms: Paradigm Shifts and New Technologies for Research, Monitoring, and Management. Annual Review of Marine Science 4: 143–176. doi:10.1146/annurev-marine-120308-081121.

Anglés S, Jordi A, Garcés E, Basterrtxea G, Palanque A (2010) Alexandrium minutum resting cysts distribution dynamics in a confined site.Deep Sea Research II 57:210-221. doi:10.1016/j.dsr2.2009.09.002

Argote-Espinoza M. (1991) Wind-induced circulation in Todos Santos bay, BC, Mexico. Atmósfera 4: 101–115.

Arthur Edelstein, Nenad Amodaj, Karl Hoover, Ron Vale, and Nico Stuurman (2010), Computer Control of Microscopes Using μManager. Current Protocols in Molecular Biology 14.20.1-14.20.17

Bissett WP, Schofield O, Glenn S, Cullen JJ, Miller WL, et al. (2001) Resolving the Impacts and Feedback of Ocean Optics on Upper Ocean. Oceanography 14(3): 30–53.

Burkholder J, Azanza R, Sako Y (2006) The ecology of harmful dinoflagellates. In: Granéli E, Turner J, editors. Ecology of Harmful Algae. Berlin Springer pp. 53–65.

Carpenter E, and Chang J (1988) Species-specific phytoplankton growth rates via diel DNA synthesis cycles I. Concept of the method. Marine Ecology Progress Seies 43:105-111.

Cetta C., Anderson, D (1990) Cell cycle studies of the dinoflagellates Gonyulax polyedra Stein and Gyrodinium uncatenum Hulburt during asexual and sexual reproduction. J. Exp. Mar. Biol. Ecol 135:69-84.

Checkley DM, Barth J a. (2009) Patterns and processes in the California Current System. Progress In Oceanography 83: 49–64. doi:10.1016/j.pocean.2009.07.028.

Cheriton O, McManus M, Stacey M, Steinbuck J (2009) Physical and biological controls on the maintenance and dissipation of a thin phytoplankton layer. Marine Ecology Progress Series 378: 55–69. doi:10.3354/meps07847.

Cullen J (1985) Diel vertical migration by dinoflagellates: Roles of carbohydrate metabolism and behavioral flexibility. Contrib Mar Sci 27: 135–152.

Cullen J, MacIntyre J (1998) Behavior, physiology and the niche of depth-regulating phytoplankton. In Physiological Ecology of Harmful Algal Blooms, D. M. Anderson, A. D. Cembella and G. M. Hallegraeff, eds. Berlon Springer pp. 559–58

Cullen JJ, Horrigan SG (1981) Effects of nitrate on the diurnal vertical migration, carbon to nitrogen ratio, and photosynthetic capacity of the dinoflagellate Gymnodium splendens. Marine Biology 62: 81–89.

Dagenais-Bellefeuille S, Bertomeu T and Morse D (2008). S-phase and M-phase timing are under independen circadian control in the dinoflagellate *Lingulodinium*. Jounal of Biological Rhytms 23(5):400-408.

Dekshenieks M, Donaghay P, Sullivan J, Rines J, Osborn T, et al. (2001) Temporal and spatial occurrence of thin phytoplankton layers in relation to physical processes. Marine Ecology Progress Series 223: 61–71. doi:10.3354/meps223061.

Dietrich G, Kalle K, Krauss W, Siedler G (1975) Allgemeine Meereskunde, eine Einführung in die Meereskunde. Berlin: Gebrüder Borntraeger. p. 593.

Doblin M, Thompson P, Revill A, Butler E, Blackburn S, et al. (2006) Vertical migration of the toxic dinoflagellate Gymnodinium catenatum under different concentrations of nutrients and humic substance in culture. Harmful Algae 5: 665–677. doi:10.1016/j.hal.2006.02.002.

Donaghay PL, Osborn TR (1997) Toward a theory of biological-physical control of harmful algal bloom dynamics and impacts. Limnology and Oceanography 42: 1283–1296. doi:10.4319/lo.1997.42.5_part_2.1283.

Donlon C, Minnett P, Gentemann C, Nightingale T, Barton I, et al. (2002) Toward improved validation of satellite sea surface skin temperature measurements for climate research. Journal of Climate 15:353–369.

Dortch Q, Maske M (1982) Dark uptake of nitrate and nitrate reductase activity of a red-tide population off Peru. Marine Ecology Progress Series 9: 299–303.

Fiedler PC (2010) Comparison of objective descriptions of the thermocline. Limnology and Oceanography Methods 8:313-325. doi: 10:4319/lom.2010.8.313.

Figueroa, R. I., Garcés, E., and Bravo, I. (2010). The use of flow cytometry for species identification and life-cycle studies in dinoflagellates. Deep Sea Research Part II: Topical Studies in Oceanography, 57(3-4), 301-307.

Franks P (1992) Sink or swim: accumulation of biomass at fronts. Marine Ecology Progress Series 82:1-12.

Gentemann CL, Donlon CJ, Stuart-Menteth A, Wentz FJ (2003) Diurnal signals in satellite sea surface temperature measurements. Geophysical Research Letters 30:2–5.

Gentemann CL, Minnett PJ (2008) Radiometric measurements of ocean surface thermal variability. Journal of Geophysical Research 113: 1–13. doi:10.1029/2007JC004540.

Gentemann CL, Minnett PJ, Ward B (2009) Profiles of ocean surface heating (POSH): A new model of upper ocean diurnal warming. Journal of Geophysical Research 114: 1–21. doi:10.1029/2008JC004825.

Gentien, Patrick, Donaghay Percy, Yamazaki Hidekatsu, Raine Robin, Reguera Beatriz OT (2005) Harmful algal blooms in stratified environments. Oceanography 18: 172–183.

Gilbert P, Burkholder J (2006) The complex relationships between increases in fertilization of the earth, coastal eutrophication and proliferation of harmful algal blooms. In: Granélli E, Turner JT, editors. Ecology of harmful algae. Berlin: Springer Berlin pp. 341–354.

Gilbert PM, Anderson D, Gentien P (2005) The global, complex phenomena of harmful algal blooms. Oceanography 18: 136–147. doi:10.5670/oceanog.2005.49.

Gisselson L.A, Granéli E and Carlsson P (1999). Using cell cycle analysis to estimate in situ growth rate of the dinoflagellate Dinophysis acuminate: drawbacks of the DNA quantification method. Marine Ecology Progress Series 18455-62.

Haase AT, Eggleston DB, Luettich R a., Weaver RJ, Puckett BJ (2012) Estuarine circulation and predicted oyster larval dispersal among a network of reserves. Estuarine, Coastal and Shelf Science 101: 33–43. doi:10.1016/j.ecss.2012.02.011.

Haberkorn H, Marie D, Lambert C, Soudant P (2011) Flow cytometric measurements of cellular responses in a toxic dinoflagellate, *Alexandrium minutum*, upon exposure to thermal, chemical and mechanical stresses. Harmful Algae 10:463-471.

Hallegraeff GM (1993) A review of harmful algal blooms and their apparent global increase. Phycologia 32: 79–99. doi:10.2216/i0031-8884-32-2-79.1.

Hartmann, D. (1994), Global Physical Climatology. 411 pp., Burlington Academic Press, MA.

Heaney SI, Eppley RW (1981) Light, temperature and nitrogen as interacting factors affecting diel vertical migrations of dinoflagellates in culture. Journal of Plankton Research 3(2):331-343.

Hernández-Walls R (1986) Circulación inducida por viento en la zona costera. Tesis de Licenciatura, UABC.

Hinder S, Hay G, Edwards M, Roberts E, Walne A, et al. (2012) Changes in marine dinoflagellate and diatom abundance under climate change. Nature climate change 2: 271–275. doi:doi:10.1038/nclimate1388.

Hyder P, Simpson JH, Xing J, Gille ST (2011) Observations over an annual cycle and simulations of wind-forced oscillations near the critical latitude for diurnal–inertial resonance. Continental Shelf Research 31: 1576–1591. doi:10.1016/j.csr.2011.06.001.

Ji R, Franks P (2007) Vertical migration of dinoflagellates: model analysis of strategies, growth, and vertical distribution patterns. Marine Ecology Progress Series 344: 49–61. doi:10.3354/meps06952

Jochem F and Meyerdierks D (1999). Cytometric measurments of the DNA cell cycle in the presence of chlorophyll autofluorescence in marine eukaryotic phytoplankton by the blue-light excited dye YOYO-1. Marine Ecology Progress Series 185:301-307.

Jordi A, Basterretxea, Casas B, Anglés, Garcés E (2008) Seiche-forced resuspension events in a Mediterranean harbour. Continental shelf research 28(4-5):505-515. doi.org/10.1016/j.csr.2007.10.009

Juhl A, Latz M (2002) Mechanisms of fluid shear-induced inhibition of population growth in a red-tide dinoflagellate. Journal of phycology 694: 683–694

Kamykowski D, Yamazaki H (1997) A study of metabolism-influenced orientation in the diel vertical migration of marine dinoflagellates. Limnology and Oceanography 42(5): 1189–1202.

Kamykowski D, Zentara S (1977) The diurnal vertical migration of motile phytoplankton through temperature gradients. Limnology and Oceanography 22(1): 148–151.

Kaplan DM, Largier JL, Navarrete S, Guiñez R, Castilla JC (2003) Large diurnal temperature fluctuations in the nearshore water column. Estuarine, Coastal and Shelf Science 57: 385–398. doi:10.1016/S0272-7714(02)00363-3.

Katano T, Yoshida M, Yamaguchi S, Hamada T, Yoshino K, et al. (2011) Diel vertical migration and cell division of bloom-forming dinoflagellate Akashiwo sanguinea in the Ariake Sea, Japan. Plankton Benthos Res 6(2):92-100.

Kirpatrick B, Fleming L, Backer L, Bean J, Tamer R, et al. (2006) Environmental exposures to Florida red tides: Effects on emergency room respiratory diagnoses admissions. Harmful Algae2 5: 526:533. doi:10.1016/j.hal.2005.09.004.

Kudela RM, Pitcher GC, Probyn T, Figueiras F, Moita T, et al. (2005) Harmful algal blooms in coastal upwelling systems. Oceanography 18: 184–197. doi:10.5670/oceanog.2005.53.

Lewitus AJ, Horner R a., Caron D a., García-Mendoza E, Hickey BM, et al. (2012) Harmful algal blooms along the North American west coast region: History, trends, causes, and impacts. Harmful Algae 19: 133–159. doi:10.1016/j.hal.2012.06.009.

Linacre L, Landry M, Cajal-Medrano R, Lara-Lara R, Hernandez-Ayon J.M, Mouriño-Pérez R, García-Mendoza E, Bazán-Guzmán C (2012) Temporal dynamics of carbon flow through the microbial plankton community in a coastal upwelling system off northern Baja California, Mexico. Marine Ecology Progress Series 461:31-46.

Lucas AJ, Pitcher GP, Probyn TA, Kudela R (2012) The influence of diurnal winds on phytoplankton dynamics in a coastal upwelling system. Deep-Sea Research II: Topics in Oceanography: in press.

MacIntyre J, Cullen J, Cembella A (1997) Vertical migration, nutrition and toxicity in the dinoflagellate Alexandrium tamarense. Marine Ecology Progress Series 148: 201–216.

Marie D, Partensky F, Jacquet S, and Vaulot D (1997). Enumeration and cell cycle analysis of natural population of Marine Picoplankton by flow cytometry using the nucleic acid stain SYBR Green I. Applied and Environmental Microbiology 63(1):186-193.

Maske H, Ochoa J, Almeda C, Carrasco Avendaño A (2012) Free-rising, tethered CTD profiler: increased vertical resolution and near surface profiling. Limnology and Oceanography Methods 10(7):475–482. doi:10.4319/lom.2012.10.475.

McDuff RE, Chisholm SW (1982) The calculation of in situ growth rates of phytoplankton populations from fractions of cells undergoing mitosis: A clarification. Limnol Oceanogr 27:783- 788

McManus MA, Woodson CB (2012) Plankton distribution and ocean dispersal. The Journal of experimental biology 215: 1008–1016. doi:10.1242/jeb.059014.

McManus MA, Woodson CB (2012) Plankton distribution and ocean dispersal. The Journal of experimental biology 215: 1008–1016. doi:10.1242/jeb.059014.

Minnett PJ (2003) International Journal of Remote Radiometric measurements of the sea-surface skin temperature : the competing roles of the diurnal thermocline and the cool skin. International Journal of Remote Sensing 24: 5033–5047. doi:10.1080/0143116031000095880

Minnett PJ, Smith M, Ward B (2011) Measurements of the oceanic thermal skin effect. Deep Sea Research Part II: Topical Studies in Oceanography 58: 861–868. doi:10.1016/j.dsr2.2010.10.024.

Noh Y, Goh G, Raasch S, Gryschka M (2009) Formation of a Diurnal Thermocline in the Ocean Mixed Layer Simulated by LES. Journal of Physical Oceanography

39: 1244–1257. doi:10.1175/2008JPO4032.1

Nuñez R (2001) DNA measurements and cell cycle analysis by flow cytometry. Mol Biol 3(3):67-70.

Omand MM, Leichter JJ, Franks PJS, Guza RT, Lucas AJ, et al. (2011) Physical and biological processes underlying the sudden surface appearance of a red tide in the nearshore. Limnology and Oceanography 56: 787–801. doi:10.4319/lo.2011.56.3.0787.

Peña-Manjarrez JL, Helenes J, Gaxiola-Castro G, Orellana-Cepeda E (2005) Dinoflagellate cysts and bloom events at Todos Santos Bay, Baja California, México, 1999–2000. Continental Shelf Research 25: 1375–1393. doi:10.1016/j.csr.2005.02.002.

Pierce RH, Henry MS, Blum PC, Osborn SE, Cheng Y-S, et al. (2011) Compositional changes in neurotoxins and their oxidative derivatives from the dinoflagellate, Karenia brevis, in seawater and marine aerosol. Journal of plankton research 33: 343–348. doi:10.1093/plankt/fbq115.

Pineda J, Hare J, Sponaugle S (2007) Larval Transport and Dispersal in the Coastal Ocean and Consequences for Population Connectivity. Oceanography 20: 22–39. doi:10.5670/oceanog.2007.27.

Price JF, Weller R a, Schudlich RR (1987) Wind-driven ocean currents and Ekman transport. Science 238: 1534–1538. doi:10.1126/science.238.4833.1534.

Ruddick KG, De Cauwer V, Park Y-J, Moore G (2006) Seaborne measurements of near infrared water-leaving reflectance: The similarity spectrum for turbid waters. Limnology and Oceanography 51: 1167–1179. doi:10.4319/lo.2006.51.2.1167.

Shulman I, Penta B, Moline M a., Haddock SHD, Anderson S, et al. (2012) Can vertical migrations of dinoflagellates explain observed bioluminescence patterns during an upwelling event in Monterey Bay, California? Journal of Geophysical Research 117: 1–10. doi:10.1029/2011JC007480.

Simpson J (1994) Sea breeze and local winds. Cambridge University Press.234 pp

Sinclair G a., Kamykowski D (2008) Benthic-pelagic coupling in sediment-associated populations of Karenia brevis. Journal of Plankton Research 30: 829–838. doi:10.1093/plankt/fbn042.

Smayda T (1997) Harmful algal blooms: Their ecophysiology and general relevance to phytoplankton blooms in the sea. Limnology and oceanography 42: 1137–1153.

Smayda TJ (2010) Adaptations and selection of harmful and other dinoflagellate species in upwelling systems. 2. Motility and migratory behaviour. Progress in Oceanography 85: 71–91. doi:10.1016/j.pocean.2010.02.005.

Tang YZ, Dobbs FC (2007) Green autofluorescence in dinoflagellates, diatoms, and other microalgae and its implications for vital staining and morphological studies. Applied and environmental microbiology 73: 2306–2313. doi:10.1128/AEM.01741-06.

Tang YZ, Koch F, Gobler CJ (2010) Most harmful algal bloom species are vitamin B1 and B12 auxotrophs. Proceedings of the National Academy of Sciences of the United States of America 2010: 1–6. doi:10.1073/pnas.1009566107.

Tapia FJ, Pineda J, Ocampo-Torres FJ, Fuchs HL, Parnell PE, et al. (2004) High-frequency observations of wind-forced onshore transport at a coastal site in Baja

California. Continental Shelf Research 24: 1573–1585. doi:10.1016/j.csr.2004.03.013.

Tobin E, Grunbaum D, Cattolico R (2011) Pelagic-benthic transition of the harmful alga, Heterosigma akashiwo: Changes in swimming and implications for benthic cell distributions. Harmful Algae 10: 619–628.

Townsend DW, Pettigrew NR, Thomas AC (2001) Offshore blooms of the red tide dinoflagellate, Alexandrium sp., in the Gulf of Maine. Continental Shelf Research 21: 347–369. doi:10.1016/S0278-4343(00)00093-5.

Ward B (2006) Near-surface ocean temperature. Journal of Geophysical Research 111: 18. doi:10.1029/2004JC002689.

Ward B, Wanninkhof R (2004) SkinDeEP: A profiling instrument for upper-decameter sea surface measurements. Journal of Atmospheric and oceanic technology 21: 207–222.

Welschmeyer N (1994) Fluorometric of chlorophyll a in the presence of analysis b and pheopigments. Limnology and Oceanography 39(8): 1985–1992.

Yamamoto T, Okai M (2000) Effects of diffusion and upwelling on the formation of red tides Journal of Plankton Research 22: 363–380.

Supplemental information

Horizontal transport of *Lingulodinium polyedrum* during April 2010 bloom, first approach.

In this thesis, the main question was how does *Lingulodinium polyedrum* could form intensives blooms during several days if is a slow grow rate species which habits in a very dynamic space, is there any balance between growth rate and hydrographic dilution?

In order to answer this question horizontal movement of surface water was documented. In this section I will describe briefly the results obtained with one of the methods used: Todos Santos Bay images.

The principal objectives were:

- Identify from land the geographical location and extension of red tide patches
- Locate from land the distribution of the patches in relation to the where water samples were taken.
- Relate patches movement and wind direction.

Method

A digital camera (Nikon D40) was used to document the surface color of the bay during a red tide events, taking time series of images from the Telematics or Oceanology building at CICESE April 2010 (19/03/2010, 07/04/2010 and

09/04/2010). To minimize the superficial reflection (sun glint) a Polaroid filter was used to reduce surface reflectance and help with the identification of the patches and their movement. We took a picture every 5 minutes, started at 10:00 hrs to 13:00 hrs when the bloom was concentrated in the upper water. Per day about 70 images were taken.

Image processing

Nikon Electronic Format (.NEF) from the camera was converted into Tagged Image File Format (TIFF) to process each image taken. NEF is raw image files that contain all the image information captured by the camera's sensor along with the image's metadata (http://www.nikonusa.com/). Even though NEF is a lossless written compressed form, we needed a flexible, adaptable file format for handling image and data within a single file. For image processing we used ImageJ software (http://rsbweb.nih.gov/ij) and the following routine.

Recommendation: Before image possessing initiate, it's important to back up the original images, and work with a duplicate to ensure not to modify the original image.

IMAGE PROCESSING RUTINE

1. Convert each TIFF image in a RGB image.
2. Save RGB images in a different folder
3. Convert the sequence in to a stack
4. Save the stack
5. **Select area** of interest and references points
6. **Crop selection** (this action will crop all the images in the stacks, same size)
7. **Save** image cropped
8. **Convert Stacks** to image

9. In each image **Split channels** (treat each image separately)
10. **Save each image** in a new folder (red, green, blue)
11. Apply different arithmetic operation between channels (**Calculator plus plugin**)
12. In this case we use the relation between Blue to Red channel, to identify the patches. Also we used a factor to amplify the range in the histogram and increaser contrast. The operation used in the program was:

$$I2 = (i1/i2)\ X\ k_1 + k_2$$

$$K_1 = 200$$

$$K_2 = -50$$

Where

I2 is the image that is been possessing

i1= blue channel image

i2=red channel image

K_1= empirical factor

K_2= empirical baseline addition

13. Save the result image
14. Apply a LUT (Look up table) or false color to identify the red tide patches from the land and ocean. The *Image/Color/Edit LUT* command opens a "LUT Editor" which enables Look Up Table editing. The Open... and Save... buttons open previously saved LUT's and save currently open LUT's. These buttons are equivalent to the *File>Import>LUT...* and the *File>Save As...>LUT...* commands. The Invert... button inverts the current LUT. This is equivalent to the *Edit>Invert* command.

Results

To identify red tide patches different arithmetic operations were done to find the best combination. After step 10 during the image analysis different combination of division between channel's images were done to find the optimal combination.

Previous radiometric ocean color measurements of red tides in San Diego and Monterrey (Maske, unpublished data) had suggested that the red to blue ratio might increase the contrast and help to identify the surface red tide patches. So far our effort to enhance the red tide contrast sufficiently to identify the extension of the red tide patches was not successful; below in Figure 30 the red/blue processed image does not improve the identification of the red tide patches in relation to the 'true' colors.

One reason for the image time series was to localize the position of the sampling boat in relation to the red tide patches, and to define in the images the geo-location of the pixel where the boat is with this information we will be able to geo-rectify the images for a quantitative interpretation of the horizontal movement. In this sampling we could not clearly localize the boat.

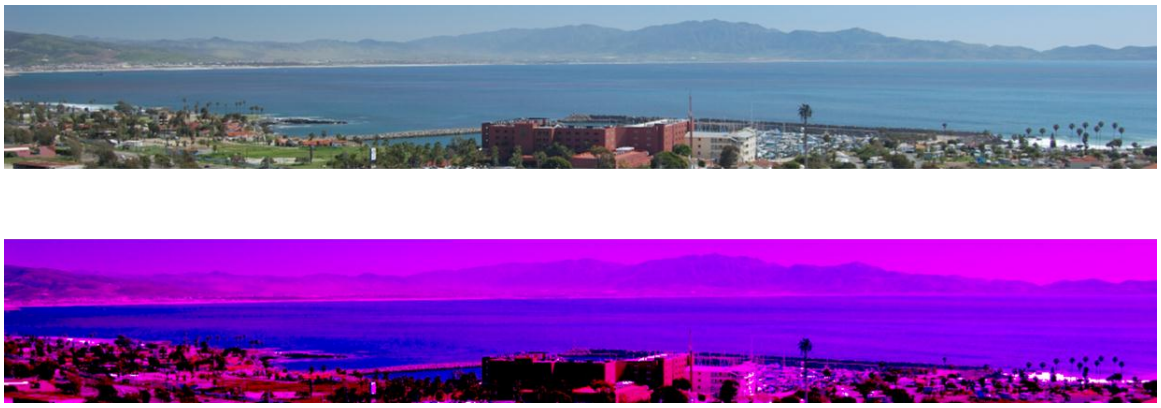

Figure 30 The 'true'color image of the bay above and the red/blue processed image below.